THE STRATIGRAPHIC AND STRUCTURAL SETTING OF THE POTRERILLOS PORPHYRY COPPER DISTRICT, NORTHERN CHILE

STEVEN F. OLSON BHP-Utah Minerals International Inc., 550 California St., San Francisco, California 94104, U.S.A.

ABSTRACT

The Potrerillos district displays major facies boundaries, records changes in the compositions of magmas from Jurassic to Oligocene time, and provides evidence that a porphyry copper deposit and associated skarn (37 Ma) formed between Jurassic-Cretaceous and Paleocene extension and Miocene compressional deformation. Pre-Jurassic granitic and metamorphic basement is overlain by Jurassic-Lower Cretaceous marine sedimentary rocks and basaltic andesite lava flows, and by Paleocene-Eocene bimodal andesite-rhyolite continental volcanic rocks. The Potrerillos district straddles major changes in facies and thicknesses of strata, between thicker, volcanic-dominant sections on the west and thinner, sedimentary-dominant sections on the east. The changes in thickness and facies are, in part, controlled by down-to-the-west normal/growth faults directly associated with the accumulation of the volcanic rocks. From Jurassic through Cretaceous time, the district occupied a back-arc setting with respect to the principal magmatic arc. Mineralized and unmineralized porphyry plutons of granodiorite to quartz monzonite composition were emplaced along the Jurassic-Cretaceous and Paleocene facies/thickness boundary between 40 and 32 Ma and represent the migration of the magmatic arc through the district. Some of the porphyry plutons were coeval with dacitic flow domes. Principal orientations of dikes *ca.* 32 Ma old indicate that the state of stress at this time was one of E-W compression (N-S extension). The major movement on reverse faults in the district and surrounding region is constrained to have occurred between 32 and 12 Ma; some Eocene movement cannot be ruled out, however. The thick volcanic-dominant western facies commonly are thrust over the thinner sedimentary-dominant eastern facies along both high-angle basement-involved reverse faults and low-moderate angle thrust faults in the sedimentary-volcanic cover. The Potrerillos porphyry copper pluton was cut and offset by a thrust fault at this time also. Basement and cover rocks record different amounts of shortening, which together, could be as high as 50% across the study area. The west-vergent reverse faults in the Potrerillos area are in part responsible for the uplift along the western edge of the Altiplano. Published rates of South America-Nazca plate convergence suggest that Paleocene bimodal volcanism occurred contemporaneously with slow rates, porphyry intrusion with increased but fluctuating rates, and compressive deformation with greatly increased rates.

Key words: Facies change, Thrust faults, High angle reverse faults, Porphyry copper, Bimodal volcanism, Potrerillos, Chile.

RESUMEN

El distrito de Potrerillos se ubica en una zona de cambios de facies mayor, registrada durante la evolución mesozoica y cenozoica del orógeno andino. Sobre el basamento granítico y metamórfico prejurásico, se disponen, en la parte oriental del distrito, rocas sedimentarias marinas jurásico-cretácicas, con intercalaciones de lavas andesítico-basálticas (cubiertas, en discordancia, por una asociación volcánica bimodal paleoceno-eocena), que gradan hacia el oeste hacia potentes secuencias volcánicas, principalmente cretácicas. El cambio de facies está controlado, en parte, por fallas normales ('down the west normal/growth faults'). Durante el Jurásico y Cretácico, el distrito ocupó una posición de tras-arco, con respecto al arco magmático andino principal. Entre 40 y 32 Ma, un conjunto de plutones porfídicos granodioríticos a cuarzo-monzoníticos (entre los cuales se incluye el pórfido cuprífero de Potrerillos) se emplazó a lo largo de la zona de cambio de facies. Algunos de ellos son contemporáneos con flujos y domos dacíticos. La orientación de los diques indica que el estado de 'stress' durante el período estuvo dominado por compresión en sentido este-oeste (extensión norte-sur). El período principal de deformación en el distrito, a través de fallas inversas, se produjo entre los 32 y 12 Ma, a pesar de que algunos movimientos podrían haber ocurrido también durante el Eoceno. Las facies occidentales, predominantemente volcánicas, están, en general, cabalgadas sobre las secuencias sedimentarias orientales, tanto a lo largo de fallas inversas de alto ángulo, que involucran al basamento, como a través de sobrescurrimientos de bajo ángulo, que afectan sólo a la cobertura. Durante la deformación el pórfido de Potrerillos fue cortado y desplazado hacia el este por una de las fallas de bajo ángulo. El acortamiento tectónico, registrado en el distrito, es diferente en el basa-

mento y la cobertura, pero la combinación de ambas componentes indica valores cercanos al 50%. Las fallas con vergencia hacia el oeste, que afectan al distrito son, en parte, responsables del alzamiento del borde occidental del Altiplano. Un examen de las velocidades de convergencia entre la placa de Nazca (y sus precursores) y la placa Sudamericana, señala que el volcanismo bimodal paleoceno tuvo lugar en un período de baja velocidad de convergencia, la intrusión de los pórfidos, con velocidades de convergencia crecientes, pero fluctuantes, mientras que la etapa de deformación compresiva coincide con un período de elevada velocidad de convergencia de placas.

Palabras claves: Cambio de facies, Fallas inversas, Cobre porfídico, Volcanismo bimodal, Potrerillos, Chile.

INTRODUCTION

For many years, the belt of porphyry copper deposits in northern Chile has been considered a metallogenetic province because of the remarkable alignment and age similarity of the host intrusions (Fig. 1; Ruiz *et al.,* 1965; Sillitoe, 1976, 1981; Clark *et al.,* 1976). Major structures in this belt, such as the West Fissure fault at Chuquicamata, are thought to have existed prior to mineralization, to have guided the emplacement of the mineralized intrusive rocks, and subsequently to have been reactivated as strike-slip or high-angle dip-slip faults (Sillitoe, 1973; Baker and Guilbert, 1987). Few district-scale studies have been sufficiently detailed, however, to determine the nature, timing, and displacement of pre-mineral movement of these structures. In addition, other features related to the setting of Chilean porphyry copper deposits, such as the composition and nature of cogenetic volcanic rocks, their time-space setting in the development of the Andean continental margin, and the localization, causes and effects of post-mineral faulting have received little attention.

Although the Jurassic-Miocene landward migration of magmatic arcs has been known to exist in some segments of northern Chile and Argentina for many years (Farrar *et al.,* 1970), there are few studies of how these arcs interacted with the Andean continental margin. Little is known about the styles and magnitudes of faulting contemporaneous with the emplacement of batholiths and major accumulations of volcanic rocks in the early stages of Andean margins. As the magmatic arc migrates through any given area, the intrusions and associated volcanic products should reflect the prevailing tectonics. This is especially true in areas of shallow porphyry intrusions where dike patterns and associated faulting are expected to be sensitive indicators of the state of stress (Heidrick and Titley, 1982; Ode, 1957; Anderson, 1951).

Whereas the styles and timing of compressional deformation of foreland areas in the Andes have been the focus of much attention (Jordan *et al.,* 1983; Jordan and Allmendinger, 1986; Mon, 1976, 1979), the styles and timing of compressional deformation in the intra-arc areas of the Chilean Andes are only known in a few areas which have

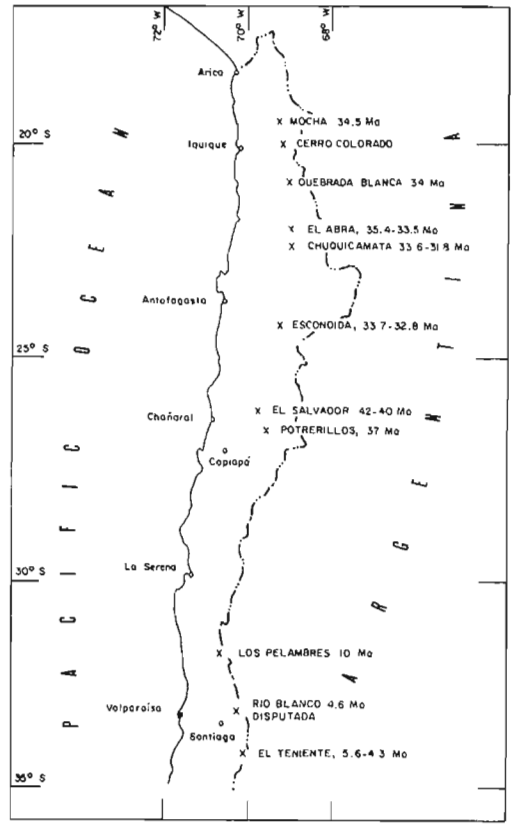

FIG. 1. Location and K-Ar ages of major porphyry copper deposits in northern Chile. Ages of porphyry copper deposits from Quirt *et al.* (1971; Mocha, Los Pelambres, Río Blanco, and El Teniente), Gustafson and Hunt (1975; El Salvador), Olson (1984; Potrerillos), Internal report, CODELCO-Chile, División Chuquicamata (no date: Chuquicamata), Ambrus (1977; El Abra), C. Alpers and G. Brimhall (written commun.; Escondida), and Hunt *et al.* (1983; Quebrada Blanca).

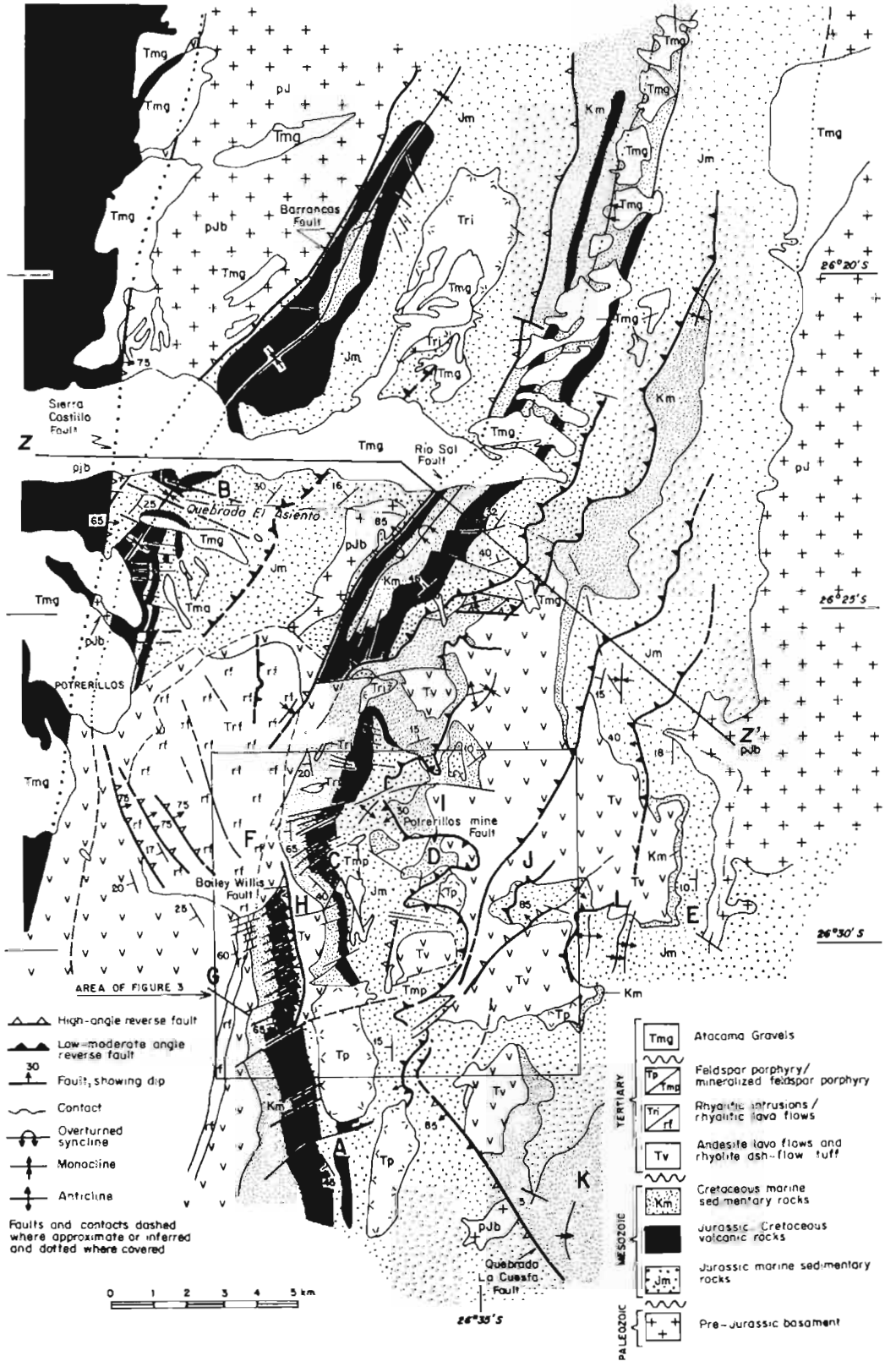

FIG. 2. Regional geologic map of the Potrerillos-Quebrada El Asiento area. Area north of Quebrada El Asiento based on Müller and Perelló (1982). Letters show locations of stratigraphic columns shown in subsequent figures. Box encloses area of figure 3. Section Z-Z' is shown in figure 13. Rocks to the west of the Sierra Castillo fault are shown as Jurassic-Lower Cretaceous marine volcanic rocks, after Naranjo and Puig (1984).

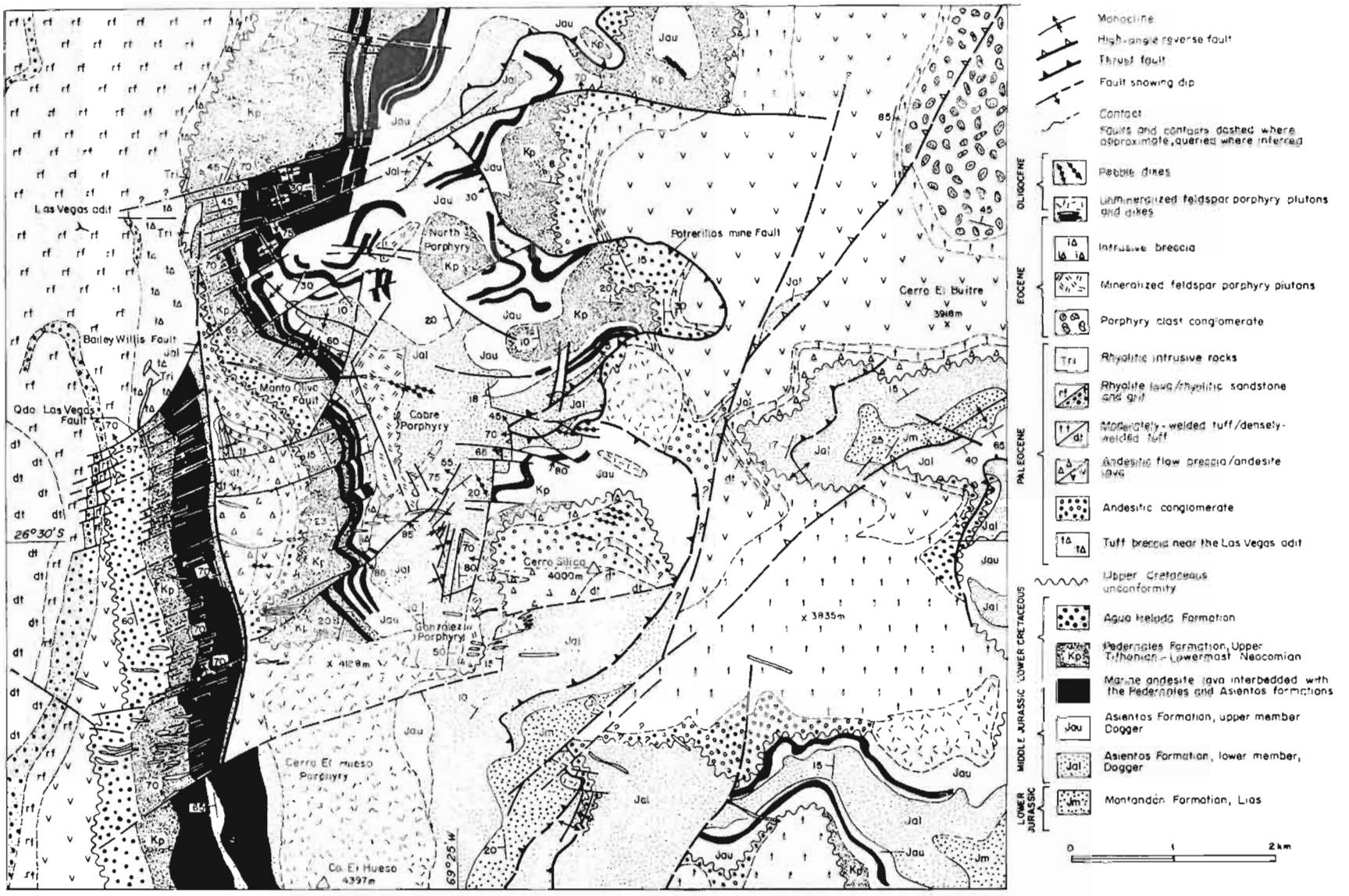

FIG. 3. Geologic map of the Potrerillos district. Location of map area is shown in figure 2. Note that the Potrerillos mine fault has cut and offset the Cobre porphyry and the porphyry copper and skarn deposit. Mapping immediately west of the Cobre Porphyry Pluton from Reed (1932).

clear, crosscutting relations (Reutter, 1974; Lahsen, 1982; Mpodozis and Davidson, 1979; Maksaev *et al.,* 1984). Shortening within the arc(s) is usually not considered in most models of Andean uplift (Cobbing, 1985; Allmendinger, 1986).

This paper first describes the stratigraphic and structural evidence for an important zone of facies and thickness changes and normal faulting that formed in the Potrerillos area (Fig. 2) in Jurassic-Cretaceous and Paleocene time, and documents the bimodal nature of volcanism up to the time of the emplacement of porphyry intrusions in Eocene-Oligocene time. It then describes the intrusion history of the district, the nature of post-mineral compressional deformation and the setting of the district in the Andean continental margin.

Total relief within the Potrerillos district (Fig. 3) including underground exposures and drill core is about 2 km, providing exposure to the wide range of geologic environments encountered in areas of shallow porphyry intrusions. During 1980 and 1981, the author spent approximately 20 months mapping in the Potrerillos district at 1:5,000 (78 km^2) and 1:2,000 (6 km^2) scales and in the surrounding area at 1:25,000 scale (200 km^2). Several kilometers of underground exposures were mapped at 1:500 and 1:1,000 scale, and several thousand meters of drill core were inspected primarily for structures and lithologic contacts. K-Ar dates were obtained in K-Ar laboratories at Stanford University and the United States Geological Survey in Menlo Park, California.

BACKGROUND

HISTORY

The richer seams and veins of the Potrerillos district were mined by selective methods as far back as 1894. William Braden acquired most of the existing claims in 1913, and sold the property to the Andes Copper Mining Company, a subsidiary of The Anaconda Copper Company, in 1916. Between 1926 and 1959, the mine produced 169 million metric tons of sulphide ore averaging 1.11% Cu and 39.2 million metric tons of oxide ore averaging 1.07% Cu (Reyes, M.: Mina Potrerillos. Internal report. CODELCO-Chile, División Salvador, 1981) by block caving methods. The mine, which was nationalized in 1971, is now the property of the Corporación Nacional del Cobre de Chile (CODELCO-Chile), the state-owned mining company. Gold and silver mineralization has recently been discovered in the district, but grades and tonnages are not available at the time of this writing.

GEOLOGIC SETTING IN NORTHERN CHILE

The Jurassic-Recent magmatic arcs and their associated sedimentary basins of the Andes of northern Chile developed in and on a pre-Middle Triassic basement that consists of Paleozoic-Triassic intrusive, volcanic, sedimentary, and metamorphic rocks (Coira *et al.,* 1982). The Potrerillos porphyry copper deposit is one of several major porphyry copper deposits of Eocene-Oligocene age in northern Chile (Fig. 1); this intrusive event appears to represent a single period of magmatism in the Andes. Farrar *et al.* (1970) demonstrated that in the Copiapó-El Salvador area, the magmatic arc migrated from Jurassic to Recent time in a stepwise fashion from the coast of Chile to the present volcanic arc along the Chilean-Argentina border, a distance of 200 to 300 km. In general, deep levels of erosion are found in the pre-Tertiary intrusions of the coast batholith (Tilling, 1976; Aguirre *et al.,* 1974), subvolcanic porphyry plutons crop out in the Eocene-Oligocene porphyry copper belt (northern Chile only; Gustafson and Hunt, 1975; Ambrus, 1977; Hunt *et al.,* 1983), and only volcanic rocks and minor subvolcanic bodies are exposed in the Miocene-Recent arc(s) (Zeil, 1979; J. Davidson, personal commun., 1987).

Most of the porphyry copper deposits in northern Chile lie within or near the Cordillera Domeyko. This discontinuous range of hills, which consists of basement blocks uplifted along high-angle reverse faults (Godoy and Davidson, 1976; Chong, 1977), appears to have been structurally active since Jurassic time (Frutos, 1974). Many of the changes in facies and stratigraphic thickness discussed in this paper coincide with the western edge of the Cordillera Domeyko.

GEOLOGIC HISTORY PRIOR TO FORMATION OF THE PORPHYRY COPPER SYSTEM

JURASSIC-CRETACEOUS MARINE SEDIMENTATION AND VOLCANISM

Jurassic marine sedimentary rocks in the Potrerillos-Quebrada El Asiento area (Fig. 4) unconformably overlie a basement consisting of metavolcanic rocks and granitic-syenitic intrusions of probable Permo-Triassic age (Pérez, 1982). The oldest marine rocks in the area consist of thin-bedded carbonaceous black marl and limestone of the Lias Montandón Formation (Pérez, 1982). The Montandón Formation is unconformably overlain by limestone, sandstone, gypsum and plagioclase-phyric basaltic andesite lava flows (Table 1, Fig. 5) of the Callovian Asientos Formation and the upper Tithonian lower Neocomian Pedernales Formation (Pérez, 1982). Red sandstone of the Lower Cretaceous Agua Helada Formation (García, 1967) caps the Mesozoic marine sequence.

From Jurassic to Lower Cretaceous time, the fu-

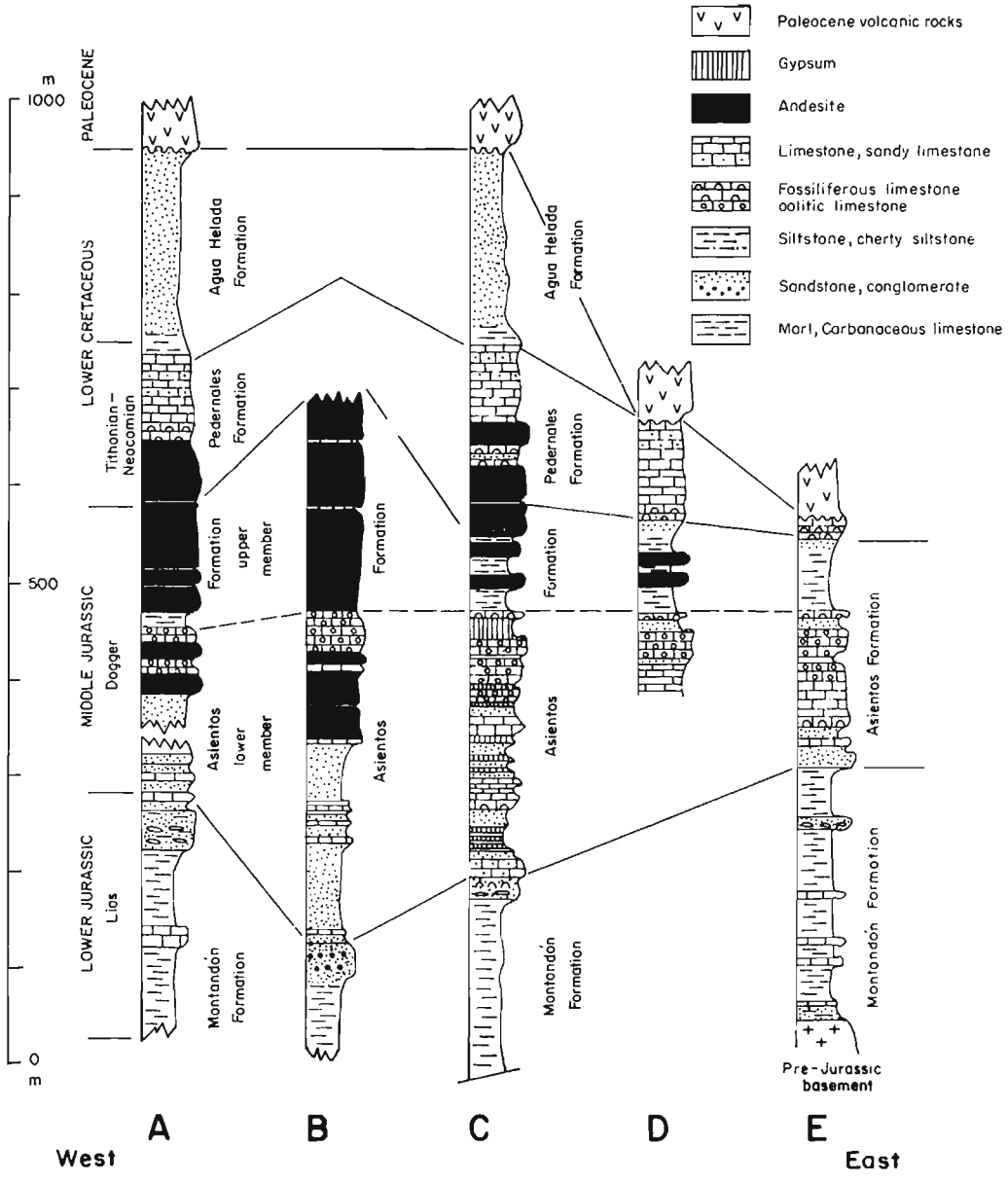

FIG. 4. Jurassic-Lower Cretaceous marine stratigraphy of the Potrerillos-Quebrada El Asiento area Column B is from Pérez (1982). Locations of columns are shown in figure 2.

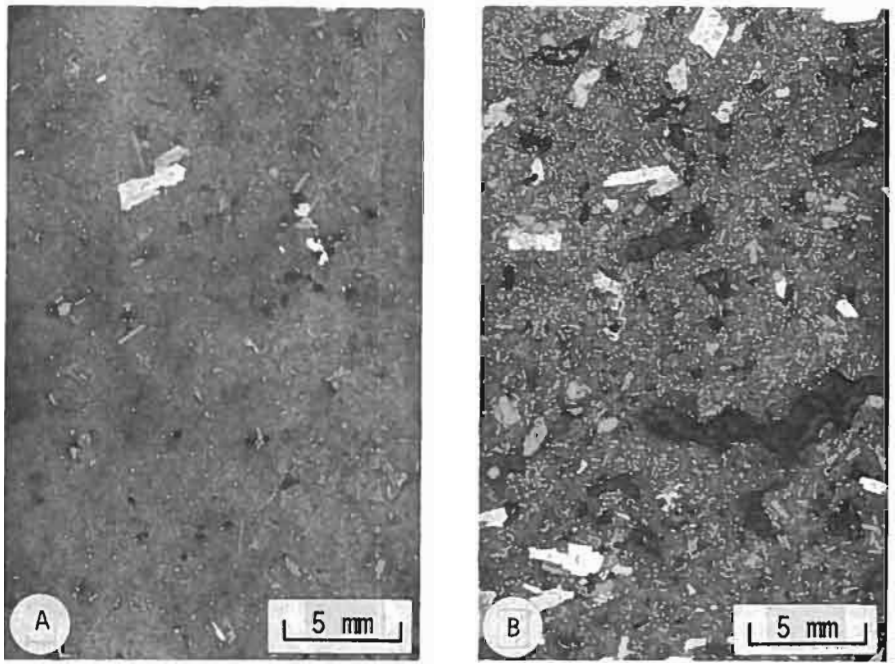

FIG. 5. Jurassic-Lower Cretaceous marine volcanic rocks A. Plagioclase-phyric basaltic andesite; B. Amygdaloidal plagioclase-phyric basaltic andesite; quartz-clorite amigdules.

TABLE 1. COMPOSITION OF JURASSIC-LOWER CRETACEOUS LAVA FLOWS

	DC-1	DC-27	DC-28	DC-29
SiO_2	50.8	53.0	48.2	55.6
TiO_2	1.89	1.83	1.78	1.73
Al_2O_3	15.12	16.31	16.78	16.53
Fe_2O_3	13.30	11.72	11.15	11.72
MnO	0.164	0.263	0.114	0.147
MgO	4.64	5.04	6.00	4.41
CaO	9.51	6.10	9.07	6.60
Na_2O	3.18	3.40	2.48	3.99
K_2O	1.06	1.64	0.63	1.78
P_2O_5	0.355	0.314	0.376	0.357
S	0.05	0.16	0.05	0.02
Cu	0.031	0.21	0.020	0.022
Total	100.1	100.01	96.65	102.91

DC-1 Basalt lava flow, 6 km ESE of Cerro El Hueso; DC-27 Basaltic andesite, Las Vegas adit, 2,051.5 m from portal; DC-28 Basaltic andesite, Las Vegas adit, 1,918 m from portal; DC-29 Basaltic andesite, Las Vegas adit, 1,850 m from portal;

Analyses by the Superintendencia de Geología, CODELCO-Chile, División Salvador. SiO_2 and P_2O_5 by wet chemical methods; remainder by atomic absorption. All iron reported as Fe_2O_3.

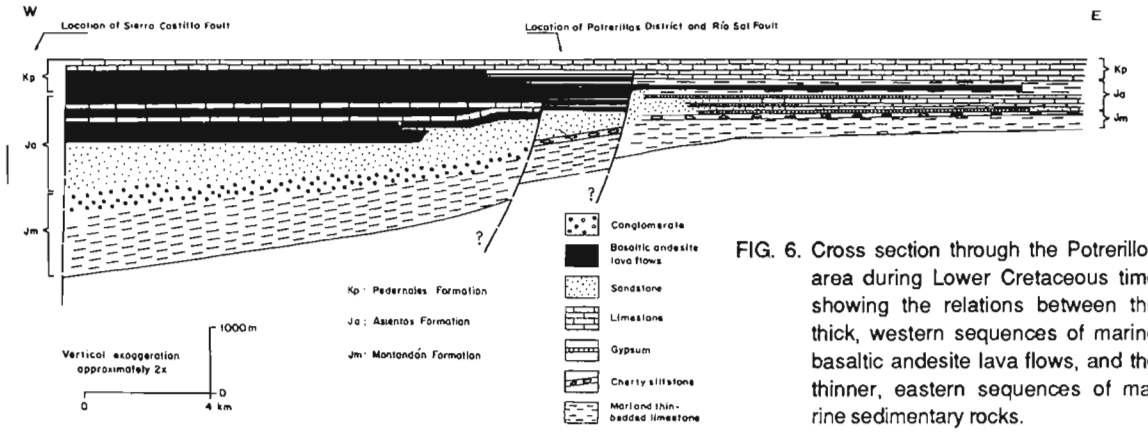

FIG. 6. Cross section through the Potrerillos area during Lower Cretaceous time showing the relations between the thick, western sequences of marine basaltic andesite lava flows, and the thinner, eastern sequences of marine sedimentary rocks.

rez, 1982). Red sandstone of the Lower Cretaceous Agua Helada Formation (García, 1967) caps the Mesozoic marine sequence.

From Jurassic to Lower Cretaceous time, the future location of the Potrerillos district coincided with a major facies and thickness change in marine sedimentary and volcanic rocks (Fig. 2-4). Thick (1.5-2 km) sequences of basaltic-andesite lava flows interbedded with sandstone and minor limestone of the Asientos and Pedernales Formations crop out on the west side of the district whereas much thinner sequences (1 km) of limestone, sandstone, gypsum and marl crop out on the east side of the district. These changes in facies and

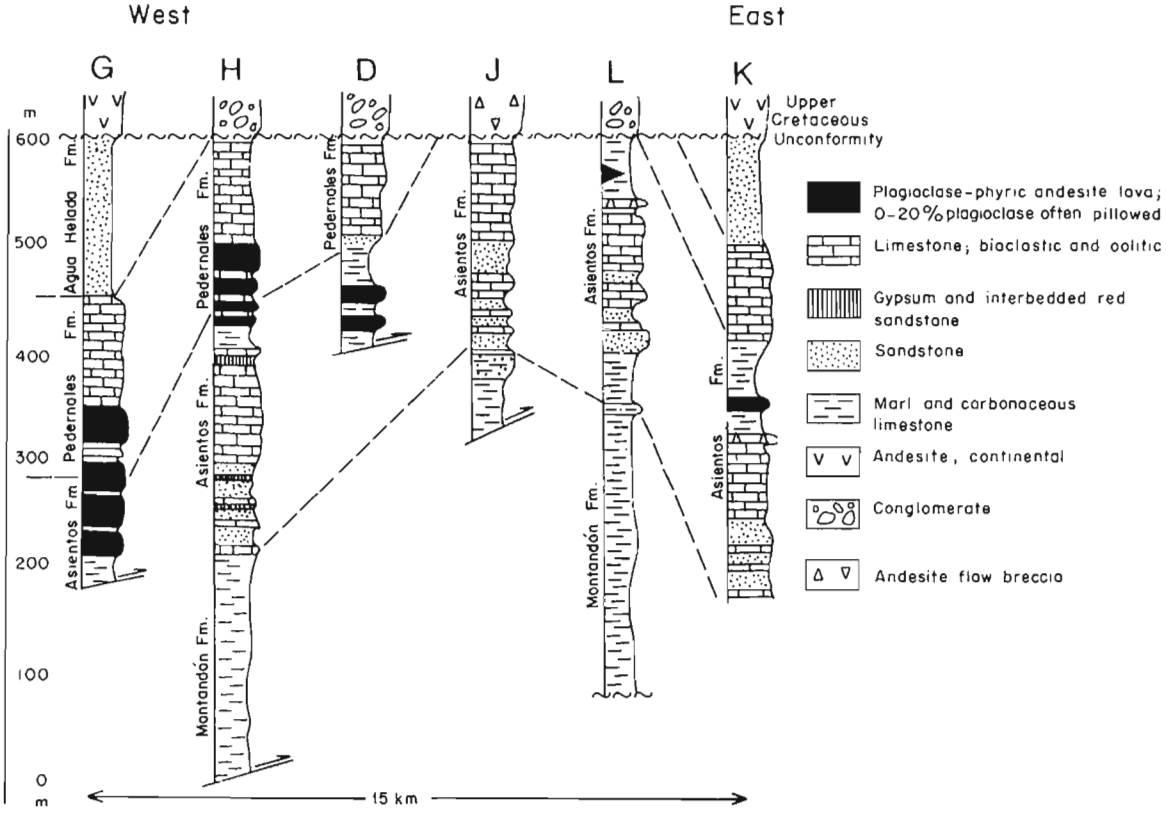

FIG. 7. Stratigraphic relations below the Upper Cretaceous unconformity. Locations of columns are shown in figure 2.

thickness can be mapped for at least 20 km to the north-northeast of the district (Müller and Perelló, 1982; Naranjo and Puig, 1984) and 50 km to the south-southeast of the district (S. F. Olson, unpubl. data).

In most cases, the changes in facies and thickness occur across high-angle reverse and thrust faults of Oligocene-Miocene age. The Río Sal fault (after Tobar, 1978) and Bailey Willis fault (after Reed, E.F.: Unpublished map of the Potrerillos district. Andes Copper Mining Co., Potrerillos, Chile. 1932; Figs. 2, 3) are two of the principal reverse faults over which the most abrupt changes in facies and thickness take place. Reconstructing these faults (this study) shows that the sedimentary-volcanic section thickens from approximately 1 km on the east to 1.5-2.0 km on the west, over a pre-thurst horizontal distance of 2-4 km. The abruptness of the changes in facies and thickness and their persistence along strike suggest that this zone was occupied by down-to-the-west normal/growth faults active during sedimentation and volcanism. A reconstructed cross section of the region at the end of Lower Cretaceous time (Fig. 6) illustrates down-to-the-west normal/growth faults bounding the thick western sequences of lava flows. Extremely thick sequences (>10 km?) of Jurassic-Cretaceous lava lie to the west of the Sierra Castillo fault (Naranjo and Puig, 1984; Mpodozis and Davidson, 1979; Muzzio, 1980) and indi-

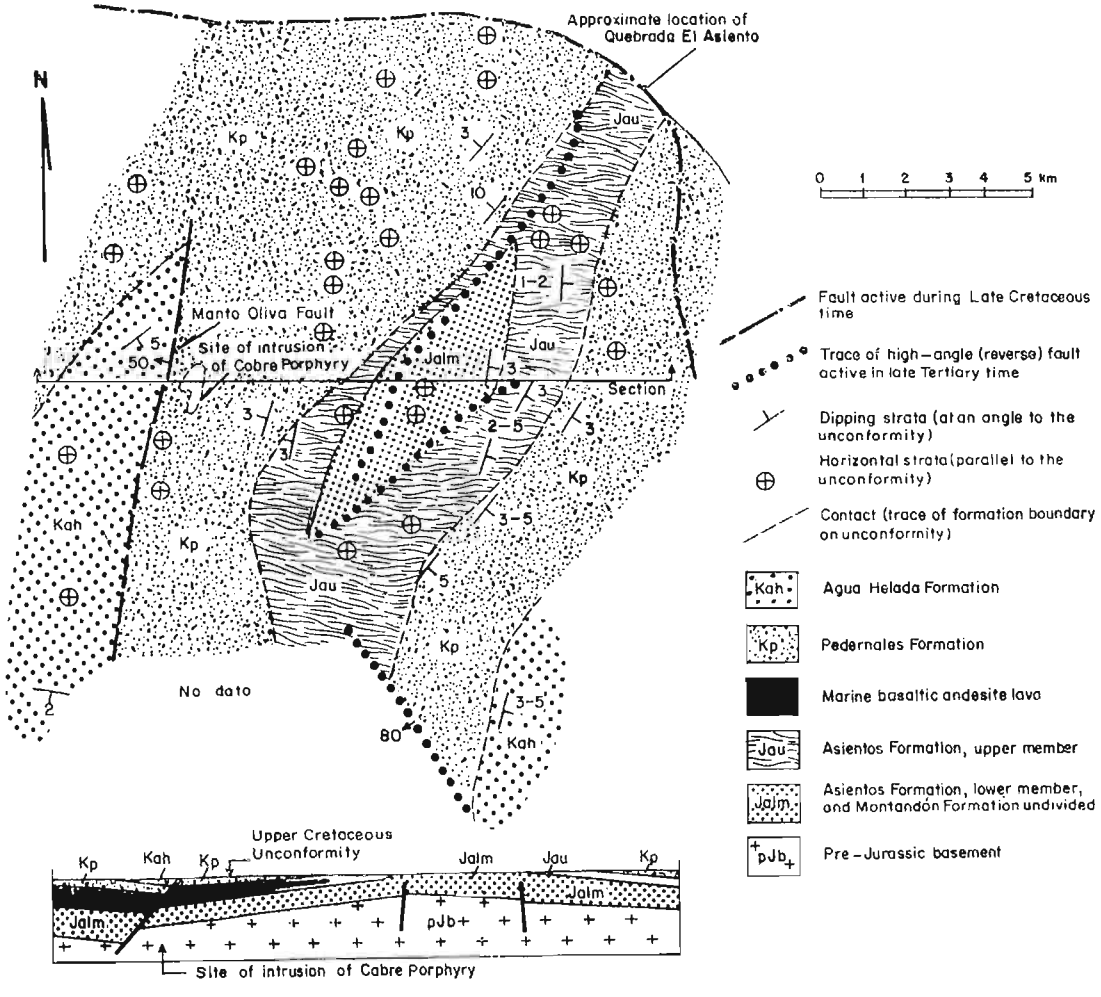

FIG. 8. Regional relations at the Upper Cretaceous unconformity. This map illustrates the distribution of formations directly below the Upper Cretaceous unconformity. Strikes and dips indicate the angle between the unconformity and stratification in the underlying rocks. Contacts indicate where a formation pinches out beneath the unconformity. The Manto Oliva fault was active during the development of the unconformity. Effects of Oligocene-Miocene reverse faulting were removed for this figure.

cate an additional westward increase in thickness of these rocks.

UPPER CRETACEOUS UNCONFORMITIES-NORMAL FAULTING AND EROSION

A major unconformity, hereafter called the Upper Cretaceous unconformity for its approximate stratigraphic position, separates the Jurassic-Cretaceous marine sedimentary-volcanic sequence from overlying Paleocene continental volcanic rocks. Stratigraphic and structural relations between the underlying marine rocks and the unconformity indicate that 200-300 m of erosion took place in Late Cretaceous time (Fig. 7) and was directly associated with movement on normal faults. Regional stratigraphic relations, however, suggest that the faulting and erosion were confined mainly to the immediate Potrerillos area (Fig. 2; Mercado, 1978, 1983).

The Manto Oliva Fault, located only 100 m west of the Potrerillos porphyry copper deposit, is one of the faults active during the development of the Upper Cretaceous unconformity (Fig. 3). Before

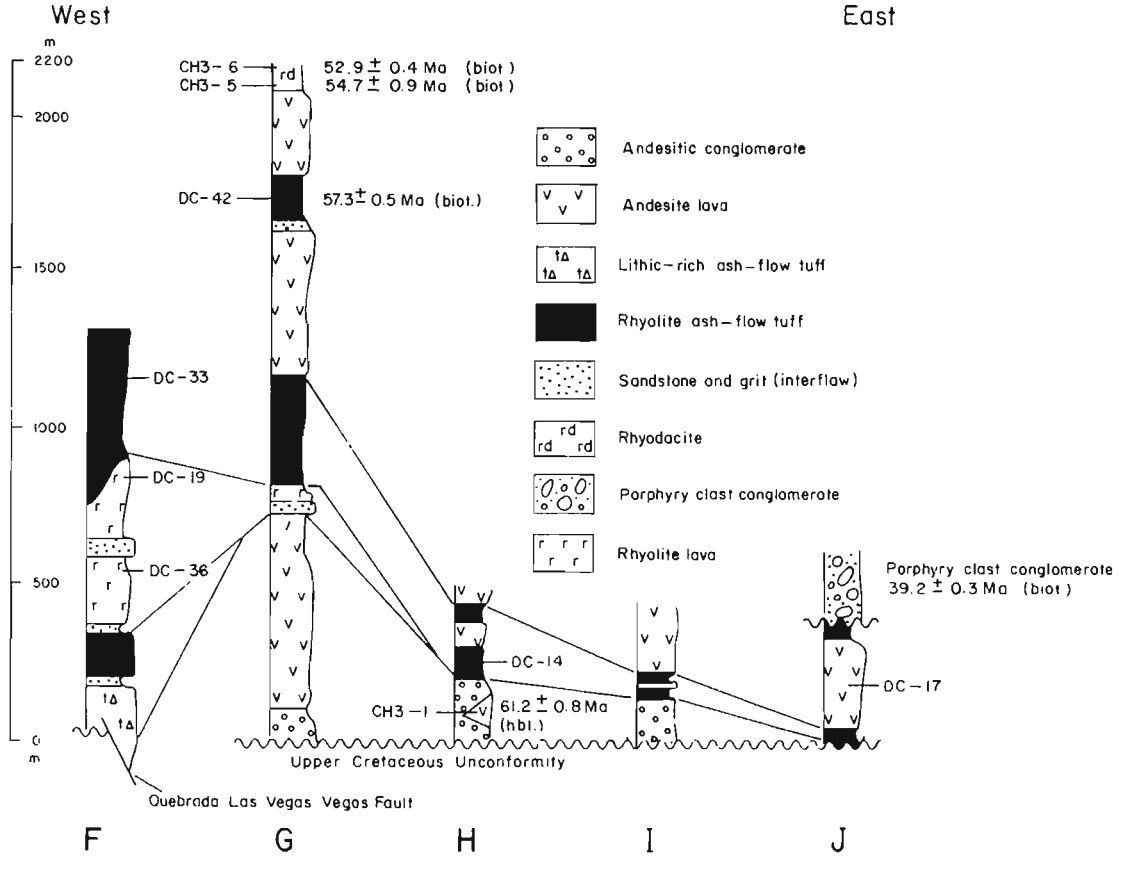

FIG. 9. Paleocene-Eocene volcanic sequences in the Potrerillos area. Locations of stratigraphic sections are shown in figure 2. Sample numbers indicate approximate locations of rocks with chemical analyses (Table 2), K-Ar ages (Table 3) and photographs (Figure 10).

TABLE 2. CHEMICAL ANALYSES OF PALEOCENE-EOCENE VOLCANIC ROCKS

	CH3-1	DC-17	DC-19	DC-14	DC-33	DC-36	CH3-5
SiO_2	51.4	51.6	66.1	74.0	74.5	73.5	70.8
TiO_2	1.12	1.45	0.87	0.15	0.16	0.12	0.33
Al_2O_3	17.4	16.4	14.5	12.8	12.7	13.0	13.7
Fe_2O_3	7.55	8.29	4.26	1.14	1.02	0.97	2.24
MnO	0.19	0.12	0.07	0.10	0.04	0.03	0.03
MgO	4.71	2.39	0.36	0.30	0.19	0.20	0.60
CaO	7.49	9.27	1.78	1.27	0.58	0.35	0.89
Na_2O	2.81	3.22	4.01	1.21	3.58	3.88	3.19
K_2O	3.73	1.91	4.76	5.21	4.52	3.91	5.40
P_2O_5	0.49	0.50	0.22	0.05	0.05	0.05	0.09
S*	N.D.	N.D.	0.06	0.01	0.08	0.07	0.06
Cu*	0.004	0.004	0.001	0.004	0.002	0.002	0.002
LOI	2.71	4.28	2.06	3.53	0.98	1.30	1.63
Total	99.6	99.43	96.99	99.77	98.67	98.38	98.97

Location of samples in Appendix
CH3-1 Plagioclase-hornblende-pyroxene-phyric andesite; DC-17 Plagioclase-phyroxene-phyric andesite; DC-19 Plagioclase-phyric dacite; DC-14 Crystal-poor rhyolite ash-flow tuff, eastern sequence; DC-33 Crystal-poor rhyolite ash-flow tuff, western sequence; DC-36 Flow banded rhyolite; CH3-5 Rhyodacite.

Analyses by U.S. Geological Survey, Branch of Analytical Chemistry, Lakewood, Colorado; by x-ray fluorescence.
* Analyses of sulfur and copper by the Superintendencia de Geología, CODELCO-Chile, División Salvador; by atomic absorption.
N.D. = not detected.
All iron reported as Fe_2O_3

the deposition of the Paleocene continental volcanic rocks, the Lower Cretaceous Agua Helada Formation was eroded from the upthrown, eastern, footwall-side of the fault, and preserved in the downdropped, western, hanging-wall side of the fault, indicating about 150 m of down-to-the-west movement between Early Cretaceous and Tertiary time. The dip of the Manto Oliva fault after removal of Oligocene-Miocene deformation, approximately 50-60°W, indicates normal movement.

Figure 8 illustrates the distribution of formations directly below the Upper Cretaceous unconformity. The map shows that stratification in the underlying rocks is subparallel to the unconformity, even though erosion at the unconformity had, in some places, removed several hundred meters of the Jurassic-Lower Cretaceous section. The Manto Oliva fault forms the contact between the downdropped Agua Helada Formation and the Pedernales Formation.

PALEOCENE CONTINENTAL BIMODAL ANDESITE-RHYOLITE VOLCANISM AND NORMAL FAULTING

During Paleocene time, basaltic, andesitic, rhyolitic, and minor dacitic volcanic rocks (Table 2) accumulated in and around the Potrerillos district. Like the Jurassic-Cretaceous volcanic rocks, the Paleocene rocks are much thicker on the west side of the district, 2-3 km, than the east, about 0.5 km (Fig. 9). Some, if not all, of the volcanic rocks accumulated on the west side of the district in fault-bounded depressions.

Radiometric age-dating of the continenta volcanic sequences indicates that the majority of the andesite and rhyolite lavas and tuff accumulated in Paleocene time (Table 3). Hornblende andesite lava near the base of the sequence yielded a K-Ar age of 61.2 ± 0.8 Ma. A biotite-bearing ash-flow tuff yielded a K-Ar age of 57.3 ± 0.5 Ma and a biotite-bearing rhyodacite lava higher in the sequence yielded K-Ar ages of 52.9 ± 0.4 and 54.7 ± 0.9 Ma.

Lithic-rich, crystal-poor rhyolite ash-flow tuff, crystal-poor rhyolite lava flows (Fig. 10, A), and interflow sandstone and conglomerate crop out between Potrerillos and the Potrerillos mine (column F, Fig. 9). This sequence is bounded on the southeast by a major down-to-the-west normal fault with about 1 km stratigraphic offset (the Quebrada Las Vegas Fault, Fig. 3) and to the north and west by faults of unknown displacement (Fig. 2). The res-

TABLE 3. K-Ar DATA FOR VOLCANIC AND INTRUSIVE ROCKS

Sample No.	Sample description and rock unit	Sample weight (gms)	K(wt%)	Radiogenic ^{40}Ar (10^{-10}mol/gm)	^{40}Ar atm (%)	Age ± 10 (Ma)
Continental volcanic rocks						
CH3-1	Hornblende, from andesite lava	0.33359	0.981 ± 0.004	1.058	33.2	61.2 ± 0.8
DC-43	Biotite, from rhyolite ash-flow tuff	0.2866	5.21 ± 0.2	1.939	23.6	57.3 ± 0.5
CH3-5	Biotite, rhyodacite lava	0.15809	6.22 ± 0.04	5.987	20.7	54.7 ± 0.4
CH3-6	Biotite, rhyodacite lava	0.34610	6.38 ± 0.04	5.941	36.9	52.9 ± 0.4
CH3-10	Biotite, from clast of porphyry-clast conglomerate	0.28669	3.51 ± 0.2	2.270	51.2	39.2 ± 0.3
Intrusions						
DC-2	Whole rock; biotite-pyroxene-plagioclase lamprophyre, 4 km east of Cerro El Hueso	2.13924	2.57 ± 0.007	1.099	34.9	45.2 ± 1.0
DC-7	Hornblende, from plagioclase-biotite-hornblende porphyry nearest to outcrop of porphyry-clast conglomerate.	0.16711	0.615 ± 0.001	1.757	80.1	40.5 ± 4.2
SNA	Biotite associated with strong potassic alteration, from fine-grained phase of Cobre porphyry.	0.20251	7.36 ± 0.02	1.648	33.2	37.0 ± 0.5
DC8	Biotite, from Cerro El Hueso Porphyry	0.3918	6.67 ± 0.03	3.709	29.3	31.8 ± 0.4
DC-9	Biotite, from Cerro El Hueso Porphyry	0.12266	6.9 ± 0.01	3.05	43.5	32.6 ± 0.5

Errors are estimated standard deviations (Cox and Dalrymple, 1967. Potassium analyses by U.S. Geological Survey, Menlo Park, California Mass Spectroscopy by J. Metz and B. Turrin. Argon extractions by S.F. Olson and B. Turrin. Sample locations in Appendix 1).

$\lambda_\varepsilon = 0.581 \times 10^{-10}$/year; $\lambda_\beta = 4.962 \times 10^{-10}$/year; $^{40}K/K = 1.167 \times 10^{-4}$.

tricted occurrence of this sequence in the region, its roughly circular outcrop pattern, and its stratigraphic and structural relations with the surrounding rocks suggest that the rhyolite flows and associated tuffs accumulated in a caldera 5-10 km in diameter located at the western edge of the district. A block-breccia (clasts up to 2 m in diameter) that lies immediately northwest of the intersection of the Bailey Willis and Quebrada Las Vegas faults may represent talus deposits formed adjacent to the caldera margin.

Abundant rhyolitic dikes, sills and irregular intrusions in the immediately surrounding country rocks appear to be cogenetic with the rhyolite flows, and are the oldest intrusive rocks in the area based on cross-cutting relationships. In many cases, the rhyolite intrudes along faults bounding the sequence of rhyolite lava flows described above. The rhyolite lavas and intrusions crop out only in the western part of the district and form part of a larger north-northeast trending belt of rhyolite and granite intrusions (Fig. 2).

Plagioclase-phyric basaltic andesite lava flows predate and post-date the rhyolite lava flows. The andesite lava flows (Figs. 10 B-D), over 300 m thick to the west of the district (column G, Fig. 9), are only 50-100 m thick to the east and are represented by andesitic conglomerate, breccia, and flow breccia (columns H, I and J, Fig. 9). North-northeast trending andesitic dikes, which cut across the rhyolite lava flows, may have been feeders for some of the andesite lavas and indicate WNW-ESE directed extension. Tobar (1978) obtained a 57 Ma K-Ar age from a lithologically similar dike in Quebrada El Asiento (Fig. 2).

Thick sequences (0.5-1.0 km) of crystal- and lithic-poor densely welded rhyolite ash-flow tuff to the west of the district (columns F and G, Fig. 9; Fig. 10, E) appear to correlate with one or two thin (50 m) persistent and compositionally similar units on the east (columns H, I and J, Fig. 9; Fig. 10, F). The thick western sequences of tuff may represent intracaldera accumulation, whereas the thin eastern sheets may represent associated outflow

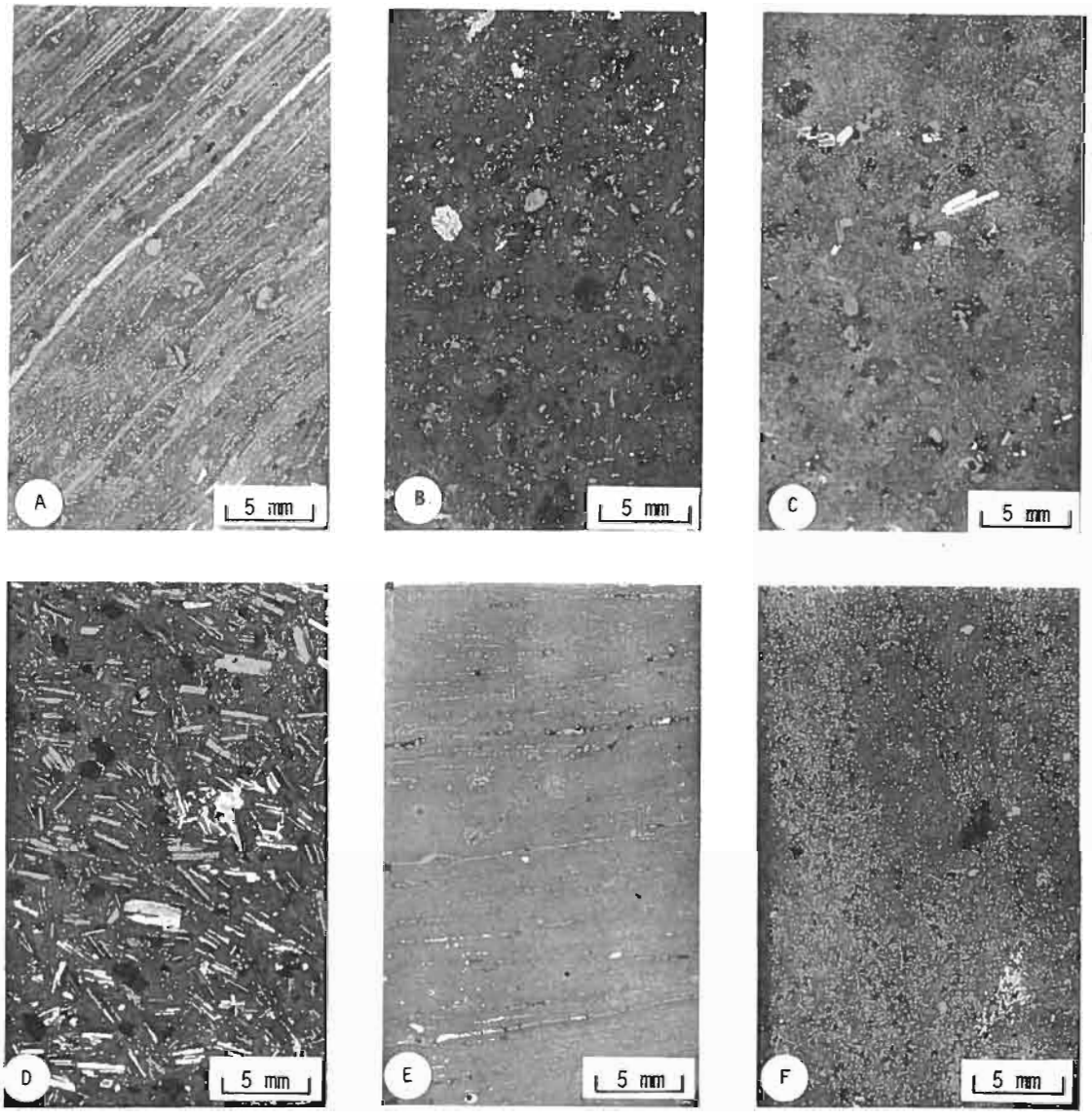

FIG. 10. Textures of Paleocene volcanic rocks in the Potrerillos district. Sample numbers indicate samples with K-Ar age date and/or chemical analyses. A. Flow-banded rhyolite, 2 km south of Potrerillos; B. Plagioclase-hornblende-pyroxene basaltic andesite; sample CH3-1; from base of Paleocene volcanic section near the Cobre porphyry; C. Phenocrysts-poor plagioclase-pyroxene andesite; sample DC-19; this is a dominant rock type in the Paleocene volcanic sequence; D. Phenocryst-rich plagioclase-pyroxene andesite, sample DC-17; this is a minor rock type in the Potrerillos area; E. Typical densely welded ash-flow tuff from the thickest accumulation of ash-flow tuff in the western volcanic sections; sample DC-33; streaks indicate rheomorphic flowage along flattened pumice lapilli, some of which show small folds; F. Typical (altered) rhyolitic ash-flow tuff from 'outflow' sheets from the eastern part of the district; sample DC-14.

facies. The thickest sequences of densely-welded tuff partially overlap the rhyolite lava flows suggesting that they accumulated in an overlapping caldera or volcano-tectonic depression. Bounding faults were probably obscured and/or remobilized by later reserve faults. One such fault, the Bailey Willis Fault, (Figs. 2, 3), lies between columns G and H of figure 9.

SUMMARY OF THE POTRERILLOS DISTRICT HISTORY PRIOR TO INTRUSION OF THE PORPHYRY COPPER SYSTEM

The first major porphyry plutons in the Potreri-

llos district were emplaced in Eocene-Oligocene time; prior to this time, the foci of igneous intrusion were to the west and had been slowly migrating to the east (Farrar *et al.,* 1970; Zentilli, 1974). The Jurassic-Paleocene volcanic rocks in the district are asymmetrically distributed and reflect the eastward migration of magmatism; the Paleocene continental volcanic rocks overlap the pinch out of the Jurassic-Cretaceous volcanic rocks. During this time, the western side of the Potrerillos district subsided more than 1.0 km relative to the east by both accumulation of volcanic rocks on the west side of the district and erosion of sedimentary rocks on the east.

The composition and structures associated with the Jurassic-Paleocene volcanic rocks suggest an extensional tectonic environment. Basaltic andesite and rhyolite constitute the dominant rock types, a bimodal assemblage indicative of extension in many environments (Hildreth, 1981). Paleocene dike orientations indicate approximate east-west extension and faults recognizable as being directly related to volcanism (Quebrada Las Vegas fault and associated structures) are normal faults. Relations at the Upper Cretaceous unconformity indicate broad uplift, normal faulting (Manto Oliva fault), and erosion.

PORPHYRY COPPER ENVIRONMENT

Numerous bodies of granodiorite to quartz monzonite porphyry (Table 4) were emplaced in the Potrerillos district between 40 and 32 Ma (Table 3) and represent the migration of the magmatic arc through the district. Their intermediate composition and crystal-rich textures represent a dramatic shift from the bimodal crystal-poor Paleocene volcanic rocks. Three of the porphyry intrusions contain copper mineralization: the Cobre porphyry and two satellite bodies, the North porphyry and the González porphyry (Fig. 3). The remainder of the intrusions, here collectively called the Cerro El Hueso porphyries because of lithologic similarity with the porphyry of Cerro El Hueso, are generally unaltered, but host intense alteration locally.

Lamprophyre

An irregular intrusion (dike and sill) of fine-grained biotite-pyroxene-plagioclase lamprophyre crops out 3 km east of Cerro El Hueso. The dike cuts across the lower-most conglomerate and ash-flow tuff of the Paleocene volcanic sequence. The rock yielded a whole rock K-Ar age of 45.2 + 1.0 Ma. With the exception of the rhyolite dikes and sills to the west of the district, it is the oldest intrusive rock in the district.

MINERALIZED PORPHYRY INTRUSIONS

Cobre Porphyry

The Cobre porphyry is a composite intrusion of several different feldspar porphyries (Reyes, M.: Mina Potrerillos. Internal Report. CODELCO-Chile, División Salvador, 1981; Parra, 1983; Reed, 1932): the 'fine-grained' porphyry, the 'intermediate' porphyry, the Secreto Porphyry, and several breccia bodies (Figs 11, A, C, D). The intrusion is elongate north-south and numerous northeast-trending dikes emanate from the eastern contact. At the present levels of exposure, the Cobre porphyry intrudes the Jurassic-Lower Cretaceous marine sedimentary-volcanic sequence in which extensive metamorphic and metasomatic aureoles and minor skarn developed (Olson, 1984).

Hypogene copper grades in the Cobre porphyry pluton in the Las Vegas level (2,983 m above sea level), range up to 1.17% Cu with significant areas over 0.8% Cu (Reyes, *op. cit.*). Information on the extent of supergene enrichment above the Las Vegas level is not available.

North Porphyry

The North porphyry (Fig. 11, B) is a NE-SW elongate feldspar porphyry intrusion about 300 m long and 100 m across. Old mine plans indicate that at depth the intrusion consists of northeast-trending anastamosing dikes. At the surface, the North porphyry intrudes the uppermost Asientos and lowermost Pedernales formations, which have been metamorphosed and metasomatized up to 500 m from the contacts. Isolated zones of quartz veins and weak copper mineralization occur in the North porphyry.

TABLE 4. INTRUSIVE ROCKS IN THE POTRERILLOS DISTRICT

Intrusion	Phenocryst Content	Groundmass Composition	Mineralization/Alteration	Dimensions at Surface	Age	Comments
North of Cerro Silica						
	Plagioclase 10-20% (2-5 mm); biotite 2-5% (3-5 mm); hornblende 1-2% (4-5 mm)	Quartz and potassium feldspar (aphanitic)	Biotite and hornblende altered to aggregates of chlorite, sericite, and limonite: locally fresh hornblende	800 m diameter, circular	40.5 ± 4.2 Ma; K-Ar; hornblende	Contemporaneous with porphyry - clast conglomerate
Cobre Porphyry Composite Pluton						
'Fine-grained' porphyry	Plagioclase 30-40% (1-3 mm); biotite 1-2% (2-4 mm); hornblende 1-2% (4-6 mm); (often replaced by aggregates of biotite)	Quartz and potassium feldspar (0.1-0.5 mm)	Early: intense quartz veining, K-silicate alteration, and cp-bn mineralization Late: pervasive sericitic alteration; py-en mineralization (Parra, 1983)	1500 m long; 500 m wide, elongate N-S	37.0 ± 0.5 Ma; K-Ar; hydrotermal biotite associated with early alteration and mineralization	Carries bulk of hypogene copper mineralization in district; data on supergene enrichment unavailable; includes abundant igneous breccias
'Intermediate' porphyry	Plagioclase 40-60% (1-6 mm); biotite 1-2% (2-4 mm); hornblende 1-2% (4-6 mm)	Quartz and potassium feldspar (0.05-0.2 mm) Aphanitic, light green	Early: weak-moderate quartz veins, K-silicate alteration, and cp-bn mineralization (Parra, 1983) Intermediate: quartz-py-mo veins near contacts Late: pervasive sericitic alteration; py-en mineralization (Parra, 1983)			Cuts across quartz veins in the fine-grained porphyry
Secreto Porphyry						
	Plagioclase 5-10% (3-6 mm); biotite 1-2% (1-2%)	Quartz, potassium feldspar, and magnetite (0.1-0.5 mm)	Fresh to weak pyrite-sericite alteration	Occupies southern part of Cobre Porhyry composite pluton		Probably associated with the unmineralized Cerro El Hueso porphyries; cuts fine-grained and intermediate porphyries
Satellite Mineralized Porphyry Intrusions						
North Porphyry	Plagioclase 40-50% (2-4 mm); hornblende 1-2% (3-6 mm)	Quartz and sericite (altered)	Hornblende partially to totally chloritized, quartz veins in central portion of stock	500 m long, 200 m wide; elongate ENE-WSW		Anastamosing dike swarm at depth
González	Plagioclase 30% (2-4 mm); quartz 5% (1-3 mm), rounded; biotite 2-3% (3-6 mm), sericitized	Quartz and potassium feldspar (0.05-0.2 mm)	Early: quartz veins, weak K-silicate alteration Late: steeply dipping limonite (after pyrite) veins with sericite selvages; pervasive sericitization	500 m long, 200 m wide; elongate N-S		Chalcocite enrichment at depth
Unmineralized Porphyry Plutons						
Cerro El Hueso	Plagioclase 10-20% (2-5 mm); biotite 1-2% (3-5 mm) quartz trace; hornblende trace		Minor areas of disseminated pyrite (0.5%); associated with a phenocryst-poor phase with a dark, aphanatic matrix; strong sericitization and silicification locally	Up to 4 km long, 2 km wide; elongate N-S; associated with E-W dike swarm	31.8 ± 0.4 and 32.6 ± 0.5 Ma; K-Ar; biotite	Found in southern part of district; probably associated with pebble dikes; miarolitic cavities or vesicles are found at the top of Cerro El Hueso elevation 4,397 m

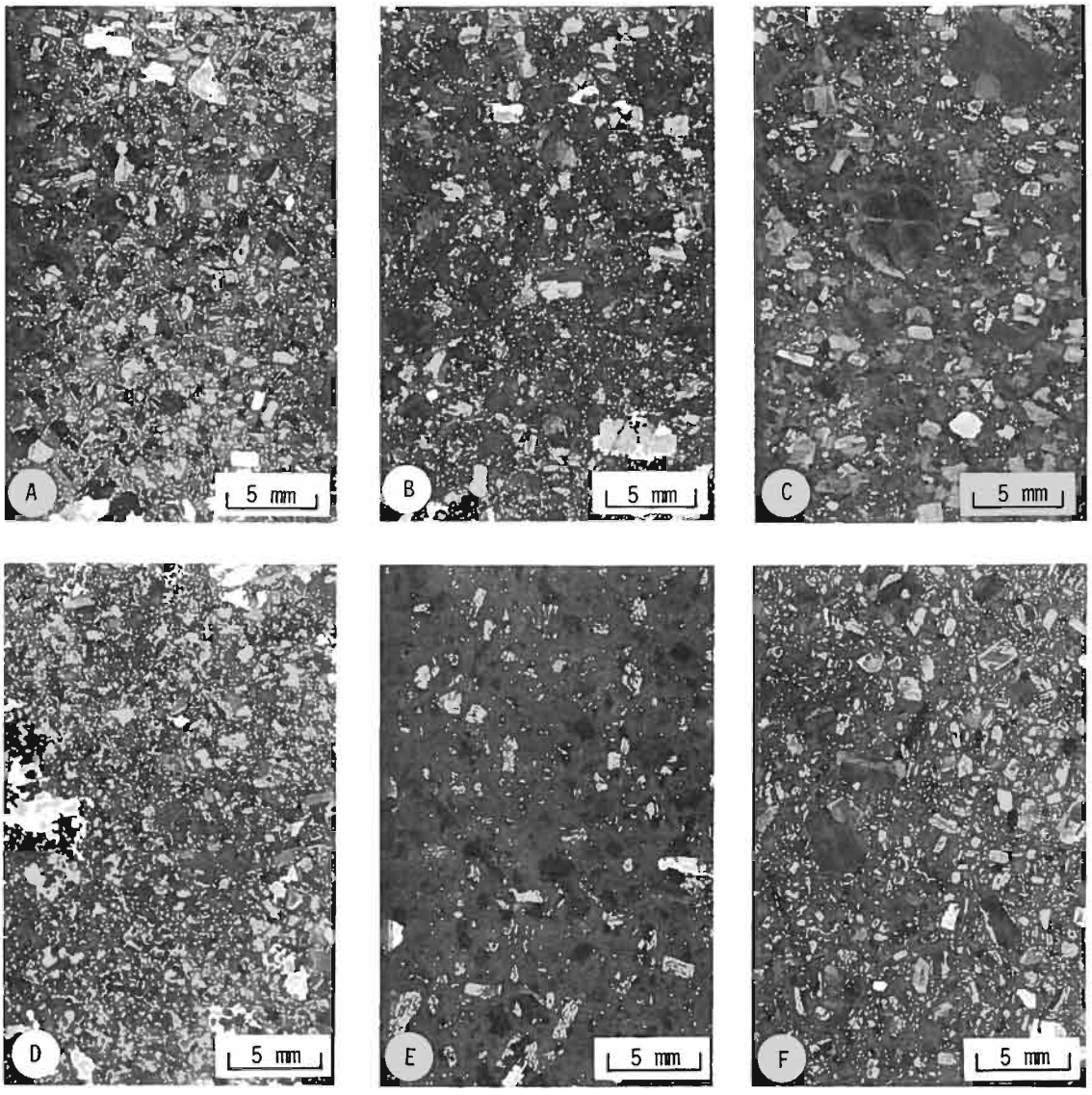

FIG. 11. Texture of Eocene-Oligocene porphyry intrusions in the Potrerillos district. Sample numbers indicate samples with chemical analyses and/or K-Ar age dates. A.'Fine-grained' porphyry, from underground exposure on the Las Vegas level (2.983 m); B. North Porphyry; sample DC-21; C. 'Intermediate porphyry', from underground exposure on the Las Vegas level; D. 'Fine-grained' porphyry with intense K-silicate alteration and quartz veins, from underground exposure on the Las Vegas level; E. Cerro El Hueso Porphyry with miarolitic cavities; sample DC-8; F. Cerro El Hueso Porphyry dike, from about 1 km east of the Cobre Porphyry.

González Porphyry

The González porphyry is the southern-most mineralized porphyry intrusion in the Potrerillos district. It is about 500 m long, 150 m wide and elongate north-south. Numerous east-west trending dike-like digitations occur along its eastern contact. The porphyry intrudes limestones and sandstone of the Asientos Formation at the surface, in which a hornfels aureole developed. The González Porphyry hosts strong sericitic alteration. Secondary copper mineralization is found in a fault zone that truncates the porphyry at depth (J. Quiroga, personal commun., 1982).

UNMINERALIZED PORPHYRY INTRUSIONS

Cerro El Hueso Porphyries

The Cerro El Hueso porphyries are the largest feldspar porphyry intrusions in the Potrerillos district. These intrusions are found in the southern part of the district, intrude the Jurassic-Cretaceous sedimentary-volcanic sequences and are elongate north-south. Narrow hornfels aureoles, in comparison to the extensive aureoles that surround the mineralized porphyries, developed around the Cerro El Hueso porphyries.

An east-west striking dike swarm originates from the northern end of the porphyry of Cerro El Hueso. The dikes, which are most abundant next to the pluton, extend up to 7 km from the pluton on either side. The Cerro El Hueso porphyry dikes (Fig. 11, F) cut the mineralized Cobre and González porphyry stocks, breccia bodies related to the Cobre Porphyry composite pluton, and Paleocene(?) andesitic dikes to the west of the district.

Miarolitic cavities or vesicles formed in the uppermost 50 m of the porphyry of Cerro El Hueso (elevation 4,397 m; Fig. 11, E). The cavities are 2-4 mm in diameter, and in some cases contain calcite. The presence of miarolitic cavities or vesicles in the highest esposure of the porphyry of Cerro El Hueso porphyries suggests that they were emplaced close to the surface, or may have been in part extrusive.

Pebble Dikes

Pebble dikes are sparse but widespread in the Potrerillos district. Within the mine area, the pebble dikes post-date copper mineralization trend, ESE-WNW, and show close spatial and temporal relations with the Cerro El Hueso porphyry dikes.The pebble dikes contain angular to rounded clasts of the surrounding wall rocks and sometimes clasts of granitic pre-Jurassic basement in a sandy, rock-flour matrix. Alteration associated with the pebble dikes is notably absent; clasts and the immediate wall rock are generally fresh and unaltered. The width of the dikes varies from almost hairline cracks to parallel-walled dikes over 2 m thick.

VOLCANIC AND TECTONIC SETTING OF THE PORPHYRY INTRUSIONS

Porphyry-Clast Conglomerate-Evidence for Cogenetic Volcanic Rocks

A conglomerate with clasts up to 1 m in diameter of plagioclase-biotite-hornblende porphyry overlies Paleocene andesite and ash-flow tuff about 5 km northeast of the Potrerillos mine. Parts of this unit are almost monolithologic and consist of angular clasts of feldspar-biotite porphyry in a matrix of similar composition; this may represent a block and ash-fall deposit derived from an extrusive dome complex. A fresh biotite mineral separate from one clast yielded a K-Ar date of 39.2 ± 0.3 Ma. The coarse clast size, intermediate composition, crystal-rich porphyry texture, and the proximity to the Eocene-Oligocene porphyry stocks of the Potrerillos district suggest that the conglomerate was derived from an unroofed stock or an extrusive equivalent of one of the stocks. A hornblende separate from the nearest feldspar porphyry stock, 3 km to the south-southwest, yielded a K-Ar age of 40.5 ± 4.2 Ma, analytically identical to the K-Ar age of the clasts.

Compression *Versus* Extension at Times of Porphyry Intrusion

Dike orientations indicate that the directions of relative extension and compression changed between Paleocene and Oligocene times. As stated earlier, north-northeast trending andesitic dikes *ca.* 57 Ma old (Tobar, 1978) indicate that the area was subjected to approximate east-west extension during Paleocene time. East-west trending dikes related to the Cerro El Hueso porphyry pluton, *ca.* 32 Ma, and related pebble dike orientations (Fig. 12) indicate that the area was under east-west compression or north-south extension) during emplacement of the younger intrusions of the district (Anderson, 1951; Ode, 1957). The general north-south trend of the major porphyry intrusions in the district probably reflects deeper structural control.

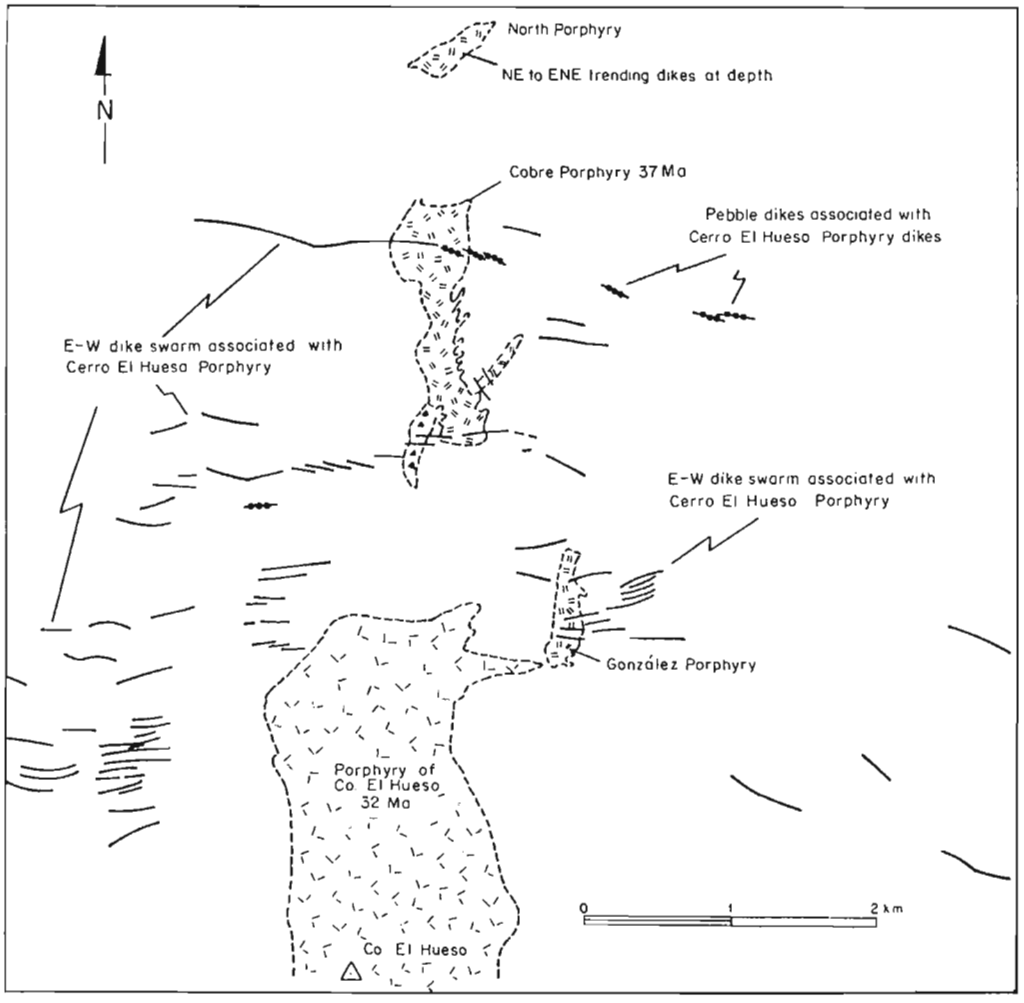

FIG. 12. East-west trending Cerro El Hueso dike swarm about 32 Ma old indicates east-west directed compression (north-south extension).

GEOLOGICAL HISTORY AFTER FORMATION OF THE PORPHYRY COPPER SYSTEM

OLIGOCENE-MIOCENE COMPRESSIONAL DEFORMATION

After the emplacement of the mineralized and unmineralized porphyry intrusions, the Potrerillos district and the surrounding area experienced a period of intense compressional deformation. Major reverse faults juxtapose the thick, western, volcanic-dominant sections against the thin, eastern, sedimentary-dominant sections (Figs. 2, 3 and 13, A).

Timing of compresive deformation is bracketed by stocks and dikes *ca.* 32 Ma old (this study) that are cut and offset by faults associated with the deformation (Fig. 3) and by ash-flow tuff and gravel 10-12 Ma old (Clark *et al.,* 1967) that mantle reverse faults on strike to the north of the Potrerillos district (Fig. 2).

STYLES OF FAULTING IN POTRERILLOS AREA

Three major types of faults formed at this time: 1. High-angle reverse faults; 2. Thrust faults; and 3. E-W to ENE-WSW trending transverse faults. Folding in the area in minor and usually developed adjacent to high-angle reverse faults.

The Potrerillos district lies at the boundary between major north-south changes in the style and trend of compressional structures. To the south, structures are dominated by NNW-SSE trending high-angle reverse faults; to the north, structures are dominated by NNE-SSW trending

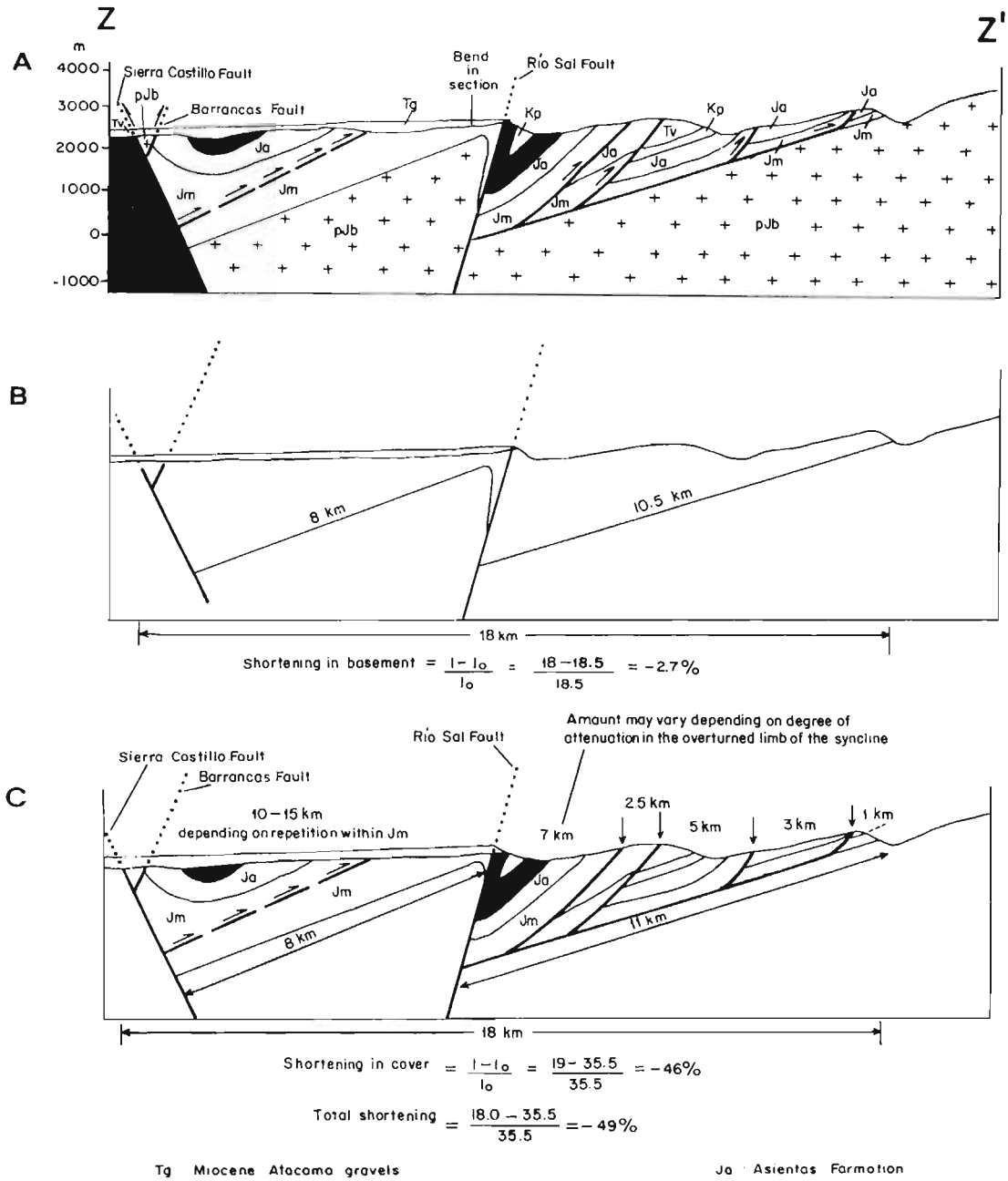

FIG. 13. A. Cross section through the Potrerillos area; see figure 2 for location of section. B. Calculation of percent shortening in basement rocks; extreme attenuation of cover rocks and apparent folding of granitic basement takes place immediately adjacent to the Río Sal faults; these phenomena are not taken into account in the calculation of shortening. C. Calculation of percent shortening in cover rocks; the bend in the cross section was made to avoid the structural complications of major transverse faults and does not appreciably change the calculated values of percent shortening (less than 5% of the given values).

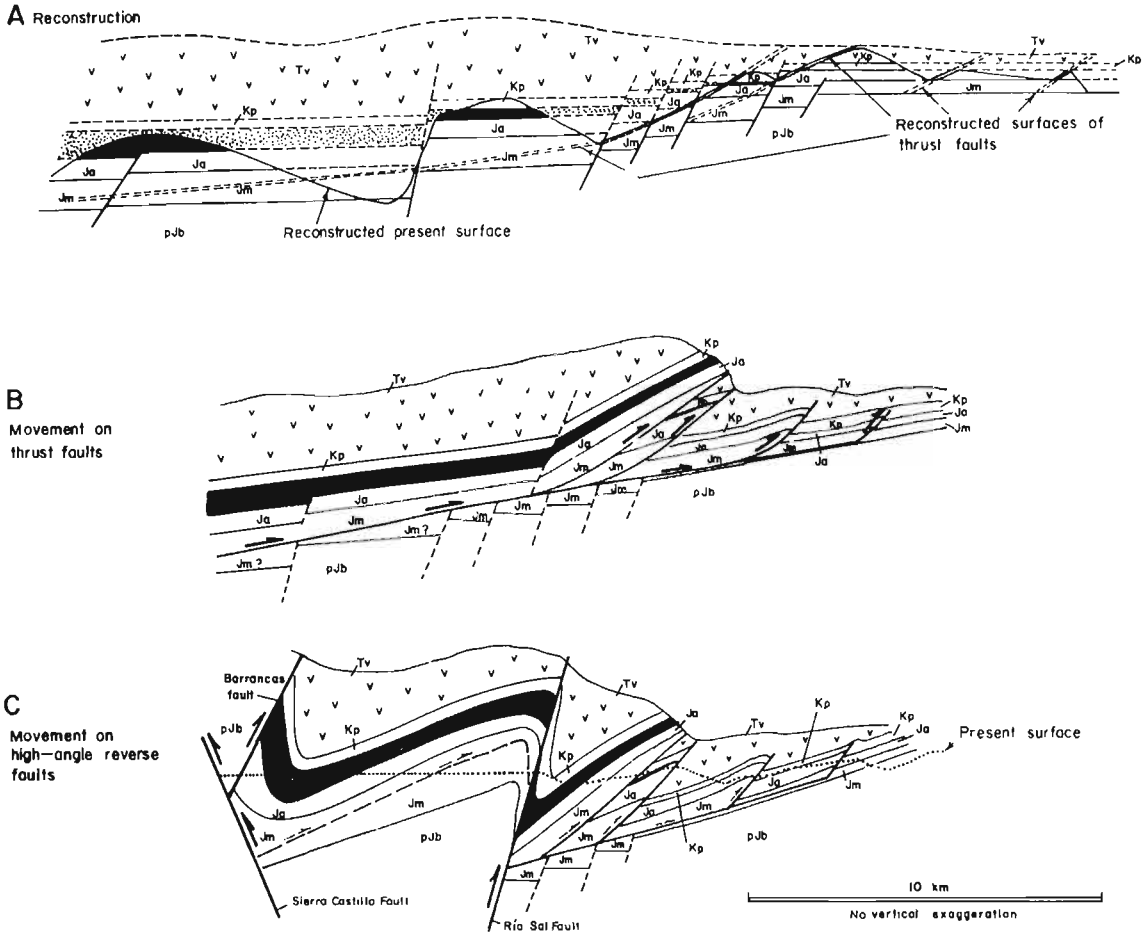

FIG. 14. Structural evolution of the thrust and high-angle reverse faults in the Potrerillos ares. Symbols as in figure 13. A. Reconstruction of the rocks now found between the Sierra Castillo fault and the eastern edge of the map area a long section Z-Z'. An attempt has been made to show the position of the thrust faults relative to the cover rocks. Contacts above the reconstructed present surface are segmented and Jurassic-Lower Cretaceous marine volcanic rocks (black) are stippled; B. Movement on thrust faults that transported about 10 km of cover rocks into the map area and may have been responsible for the initial westward tilting of the basement. C. Movement on high-angle reverse faults.

high-angle reverse faults, thrust faults, and transverse faults. This bend in strike of the high-angle reverse faults coincides with the bend in strike of the changes in facies and thicknesses of the Jurassic-Cretaceous marine-volcanic sequence.

High-Angle Reverse Faults

High-angle reverse faults are the most important through-going structures in the area surrounding the Potrerillos district (Fig. 2). Most of the faults are east-vergent and involve both the pre-Jurassic basement and the Jurassic-Paleocene sedimentary and volcanic cover. These faults dip steeply to the west, juxtapose older rocks on the west against younger rocks on the east, and often display more than 1,000 m of apparent dip-slip displacement. The Sierra Castillo fault (after Tobar, 1978), found to the northwest of the district (Fig. 2), is an important exception, however; it is a west-

vergent high-angle reverse fault with about 2 km apparent dip-slip displacement (Perelló and Müller, 1984). The Sierra Castillo fault forms the western boundary of the Cordillera Domeyko in the Potrerillos area.

Where exposed, the pre-Jurassic basement contact dips consistently 10-20 degrees to the west and has apparently been tilted between major high-angle reverse faults. The amount of shortening associated with this tilting and faulting is probably not more than 3% (Fig. 13, B).

Thrust Faults

Thrust faults are best developed from the Potrerillos district northward (Figs. 2, 3). At the present levels of exposure, the thrust faults involve only rocks of the Jurassic-Paleocene sedimentary-volcanic cover. The major thrust faults are all east-vergent, with displacements estimated between 1 and 2 km. The faults are subparallel (5-10 degrees) to bedding in marls and cut moderately to steeply (25-30 degrees) up-section in limestones and sandstone units. In areas of intense thrust faulting, dips of the cover rocks vary between 20 and 70 degrees west because: 1. The basement has been tilted an additional 20 degrees west beneath the thrust plates; and 2. Ramp anticlines in the upper plates of thrust faults increased the westward dip in some places (J. Skarmeta, personal commun., 1985).

The Cobre porphyry pluton and associated skarn were cut and offset by a major thrust fault, the Potrerillos mine fault (Fig. 3). Drillhole data indicates that the stock was displaced about 1.5 km to the east-southeast, consistent with the displacement of sedimentary horizons on the surface and with the orientations of mullions and striations on fault surfaces on the Las Vegas level.

The amount of shortening in the cover by thrust faults and folding in the Potrerillos-Quebrada El Asiento area is about 46% (Fig. 13). As stated earlier, the amount of shortening due only to the basement-involved high-angle reverse faults and associated tilting is probably not more than 3%. Together, the amount of shortening in the cover and basement rocks is probably about 50% (Fig. 13, C).

Sequence of Deformation

The disparity between these various amounts of shortening calculated for basement and cover rocks suggests that the different styles of reverse faulting acted at different times during compressive deformation and that a significant amount of cover rocks were transported into the area by thrust faults. The geometry of the thrust faults with respect to the basal unconformity and the high-angle reverse faults requires that thrusting preceded movement on the high angle reverse faults. Figure 14 illustrates one possible scenario whereby thrust faults carry additional cover rocks into the area prior to movement on the high-angle reverse faults. Westward tilting of the basement at this time may have been caused by stacking of thrust plates. In the final stages of thrusting, perhaps when the thrust faults became 'locked', major movement on the high-angle reverse faults occurred.

Transverse Faults

Transverse faults in the Potrerillos area mark the inception of high-angle reverse and thrust faults and bound changes in the structural style and dips in the upper plates of thrust faults. They trend east-northeast to east-west and have apparent right-lateral and both normal and reverse offset, ranging from several meters to up to 500 m.

The intense zone of transverse faults in the Potrerillos district marks the change in structural style from NNW-SSE trending high-angle reverse faults to the south of the district, to NNE-SSW trending high-angle reverse, thrust, and transverse faults to the north. Many of the thrust faults to the north of the district begin as transverse or tear faults.

DISCUSSION

The stratigraphic, structural, and intrusive evolution of the Potrerillos district is shown in figure 15. Normal faulting contemporaneous with the accumulation of Jurassic-Cretaceous and Paleocene volcanic rocks to the west is shown as the principal means of down-to the-west subsidence.

Rhyolite intruded along some of these faults in Paleocene time. The porphyry intrusions of Eocene-Oligocene age also intruded into this zone. Some of the intrusions vented, providing the clasts for the Eocene porphyry-clast conglomerate and block breccia now found in the northeast part of the district. Compressional deformation between Late Oligocene and Miocene time reactivated the zone of earlier normal faults; the thick, western volcanic-dominant sequences were thrust over the thin, eastern, sedimentary-dominant sequences at this time. One of these thrust faults cut and offset the Cobre Porphyry pluton.

Although evidence in the Potrerillos area indicates a Late Oligocene-Miocene age for the deformation, it does not exclude the possibility for some Eocene deformation. Data from the surrounding area indicate that some compressive deformation may have taken place in Eocene or perhaps earlier time. The Eocene porphyry plutons at El Salvador intrude folded sequences of Cretaceous-Paleocene(?) andesite lava and ash-flow tuff ('Cerrillos' and 'Hornitos' formations, Gustafson and Hunt, 1975; personal observation, 1981). Here the plutons themselves do not appear to be offset by any major faults. Also, in the Quebrada Paipote-Carrera Pinto area, Mpodozis and Davidson (1979) and Sepúlveda and Naranjo (1982) found evidence for compressive deformation before the deposition of Lower Tertiary pyroclastics.

TIME, SPACE AND MAGMATIC SETTING OF THE POTRERILLOS PORPHYRY COPPER DISTRICT IN THE ANDEAN CONTINENTAL MARGIN OF NORTHERN CHILE

The mineralized and unmineralized intrusions in the Potrerillos district intruded into a long-lived zone of facies and thickness changes and associated normal faults. This zone formed contemporaneously with major accumulations of volcanic rocks and batholitic emplacement to the west of the district. This zone of faulting and changes in facies and thicknesses also marks important changes in the regional stratigraphy of the Andes of northern Chile, separating Jurassic-Cretaceous volcanic accumulations along the coast and in the central valley regions from thinner sedimentary-dominant sequences in the Cordillera de Domeyko (García, 1967; Chong, 1977). A similar facies change is also seen in Perú (Cobbing, 1985; Megard, 1978) and central Chile (Charrier, 1981), suggesting that most of the Andes underwent a similar stratigraphic and structural evolution from at least Jurassic through Cretaceous time.

The facies changes described above do not coincide with the porphyry copper belt everywhere and may not have been significant in the localization of intrusions except at Potrerillos. The geology of the Potrerillos district suggests that: 1. The porphyry copper plutons intruded between Paleocene extension and Oligocene-Miocene compression; 2. The state of stress was one of east-west compression during the intrusion of some of the porphyries; and 3. The host intrusions were of intermediate compositions, in contrast to the preceding basaltic andesite-rhyolite bimodal magmatism.

Plate tectonic reconstructions of convergence rates between the South American and Nazca plates (Pardo-Casas and Molnar, 1987) suggest that convergence was slow during Paleocene time, increased in Early Eocene time, decreased in Late Eocene-Oligocene time, and greatly increased in Miocene time in response to reorganization and faster spreading at the East Pacific Rise (Handschumacher, 1976). In the Potrerilos area, slow convergence rates in Paleocene time were contemporaneous with extension and bimodal volcanism, the fluctuating convergence rates between Early Eocene and Oligocene time were contemporaneous with porphyry intrusion, and high convergence rates during Miocene time were contemporaneous with intense compressional deformation.

MAGNITUDE AND SETTING OF COMPRESSIONAL DEFORMATION

Most of the major high-angle reverse and thrust faults which formed during late Oligocene-Miocene compressional deformation in the Potrerillos area have at least 1 km displacement. Collectively, they could be responsible for as much as 50% shortening across the map area (presently about 20 km; Fig. 2). The major through-going structures in the area are high-angle reverse faults which follow the western edge of the Cordillera de Domeyko. These faults occur throughout northern and central Chile (Reutter, 1974; Chong, 1977; Maksaev *et al.*, 1984; Mpodozis and Ramos, in press) and roughly coincide with the western edge of the Altiplano. The major west-vergent faults in the Potrerillos area (the Sierra Castillo fault) as well as

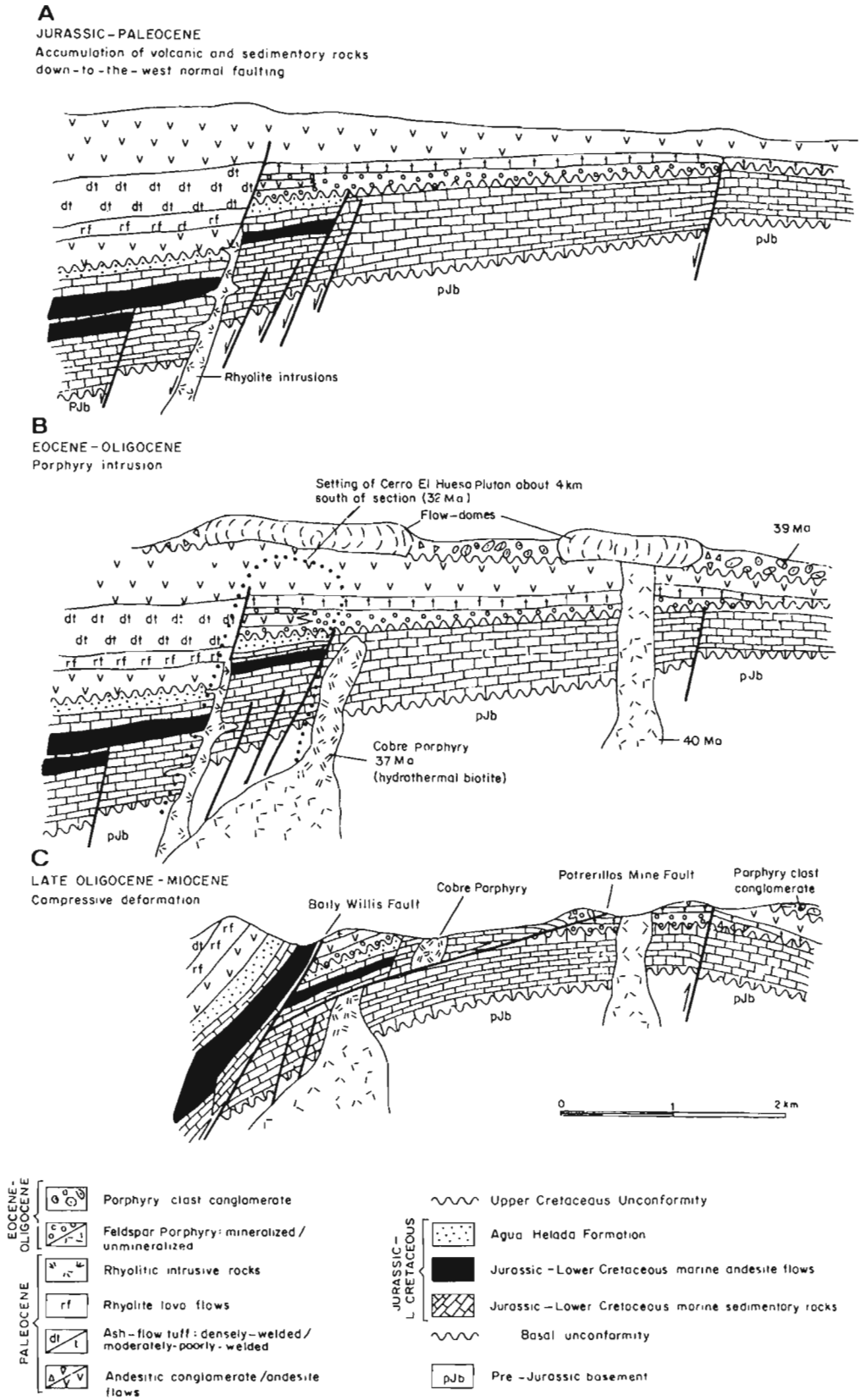

FIG. 15. Evolution of the Potrerillos district from Paleocene through Miocene time. Explanation in text.

the other faults bounding the western edge of the Altiplano could thus be viewed as part of the system of faults responsible for the uplift along the western edge of the Altiplano.

It is doubtful, however, that the shortening present in the Potrerillos area is representative of the Andes in general. Geologic maps of the Potrerillos area (Segerstrom, 1967; Mercado, 1978, 1983; Servicio Nacional de Geología y Minería, 1982) suggest that most reverse faulting is confined to relatively narrow zones separated by large areas of gently dipping strata. The deformation in the Potrerillos area appears to represent a zone of unusually high strain.

TABLE 5. CHEMICAL ANALYSES OF EOCENE-OLIGOCENE INTRUSIVE ROCKS IN THE POTRERILLOS DISTRICT

	DC-21	DC-9	DC-3	Fine*	Int*
SiO_2	64.0	67.2	60.8	65.83	61.48
TiO_2	0.59	0.34	0.49	0.51	0.65
Al_2O_3	17.1	16.2	16.5	16.07	20.24
Fe_2O_3	3,51	2.07	4.53	1.64	2.34
MnO	0.06	0.02	0.09	0.018	0.013
MgO	1.14	0.80	2.02	0.92	1.15
CaO	3.76	2.61	4.54	2.67	3.95
Na_2O	4.67	4.72	4.08	4.21	5.30
K_2O	2.18	2.16	1.73	4.15	2.30
P_2O_5	0.19	0.16	0.19	0.13	0.20
S	0.19	0.24	0.06		
Cu	0.043	0.002	0.004	0.79	0.24
LOI	1.19	1.18	4.28		
Total	98.89	98.78	99.31	97.03	97.86

DC-21 Plagioclase-hornblende granodiorite porphyry, from North Porphyry stock; DC-9 Pagioclase-biotite-hornblende-quartz monzonite porphyry, from the Cerro El Hueso Pluton; DC-3 Plagioclase-biotite-hornblende granodiorite porphyry, from porphyry stock 2 km south of Cerro El Hueso; Fine* Average of four samples of 'fine-grained' porphyry; Int* Average of four samples of 'intermediate' porphyry ('pórfido grano-grueso-feldespático' of Parra, 1983).

Analyses by U.S. Geological Survey, Branch of Analytical Chemistry, Lakewood, Colorado; by major element x-ray fluorescence. All iron reported as Fe_2O_3.

Analyses of sulfur and copper by the Superintendencia de Geología, CODELCO-Chile, División El Salvador; by atomic absorption.

* From Parra (1983)

CONCLUSIONS

The Eocene-Oligocene porphyry intrusions of the Potrerillos district were emplaced in a long-lived zone of facies sand thickness changes and associated normal faults contemporaneous with major accumulations of Jurassic-Paleocene volcanic rocks to the west. This zone was subsequently reactivated in Late Oligocene-Miocene time as a zone of intense reverse faulting. The rocks of the Potrerillos district also record the change from basaltic andesite-rhyolite volcanism in Paleocene time to intermediate composition crystal-rich porphyry intrusion in Eocene-Oligocene time. Major dike orientations suggest that the state of stress changed from approximate east-west extension in Paleocene time to east-west compression (north-south extension) at 32 Ma. The changes from Paleocene bimodal volcanism to Eocene-Oligocene porphyry intrusion and finally to Oligocene-Miocene compressional deformation are coincident with slow, fluctuating but increased, and

greatly increased convergence rates at the Nazca-South American plate boundary, respectively.

Both thrust and high-angle reverse faults in the area account for up to 50% shortening across the study area. This value is probably not representative of the shortening across the Andes, but more likely indicates a zone of especially high strain along the western edge of the Altiplano.

ACKNOWLEDGEMENTS

This paper is the outgrowth of a Ph.D. study at Stanford University supervised by Marco Einaudi (Professor of Applied Earth Science at Stanford University). John Hunt (consulting geologist of Hunt, Ware, and Proffet) and CODELCO-Chile, División Salvador initiated the author's involvement in the present study. Funding during the study was provided by CODELCO-Chile, División El Salvador and a National Science Foundation Graduate Fellowship. The geological and technical staff at El Salvador, particularly Enrique Tidy, Jorge Quiroga, and Manuel Reyes, provided excellent geologic, logistic and technical support. Brent Turrin and Jenny Metz (Stanford University) helped with the K-Ar dating. Estela Cubillos (Minera Utah de Chile) helped redraft many of the original figures for this paper. A special thanks is due to Eric Seedorff (Chevron Resources Company), who greatly improved the original manuscript and encouraged publication of this paper. Other helpful comments were given by Charles Alpers (University of California at Berkeley), James Bratt (BHP-Utah Minerals), Mary Gilzean (Minera Utah de Las Américas),John Davidson and Constantino Mpodozis (Servicio Nacional de Geología y Minería) and Richard Allmendinger (Cornell University).

REFERENCES

Aguirre, L.; Charrier, R., Davidson, J.; Mpodozis, C.; Rivano, S.; Thiele, R.; Tidy, E.; Vergara, M.; Vicente, J.C. 1974. Andean magmatism: its paleogeographic and structural setting in the central part (30-35°S) of the southern Andes. *Pacific Geology,* Vol. 8, p. 1-38.

Allmendinger, R.W. 1986. Kinematic and tectonic history of the southern margin of the Puna Plateau, northern Argentina. *Geological Society of America, Bulletin,* Vol. 97, p. 1070-1082.

Ambrus, J., 1977. Geology of the El Abra porphyry copper deposit, Chile. *Economic Geology,* Vol. 72, p. 1062-1085.

Anderson, E.M. 1951. The dynamics of faulting and dike formation. 2nd edition. *Oliver and Boyd,* 206 p. London.

Baker, R.C.; Guilbert, J.M. 1987. Regional structural control of porphyry copper deposits in northern Chile. *Geological Society of America, Abstracts with Programs,* p. 578.

Charrier, R. 1981. Mesozoic and Cenozoic stratigraphy of the Central Argentina-Chilean Andes (32-35°S) and chronology of their tectonic evolution. *Zeitblatt der Geologie und Paläontologie,* Teil I, p. 344-355.

Chong, D.G. 1977. Contribution to the knowledge of the Domeyko Range in the Andes of northern Chile. *Geologische Rundschau,* Vol. 66, p. 374-403.

Clark, A.H.; Mayer, A.E.S.; Mortimer, C.; Sillitoe, R.H.; Cooke, R.U.; Snelling, N.J, 1967. Implications of the isotopic ages of ignimbrite flows southern Atacama Desert, Chile. *Nature,* Vol. 215, p. 723-724.

Clark, A.H.; Farrar, E.; Caelles, J.C.; Haynes, S.J.; Lortie, R.B.; Zentilli, M., 1976. Longitudinal variations in the metallogenetic evolution of the central Andes: a progress report. *Geological Association of Canada, Special Paper,* No. 14, p. 23-58.

Cobbing, E.J. 1985. The tectonic setting of the Peruvian Andes. *In* Magmatism at a Plate Edge, the Peruvian Andes (Pitcher, W.S.; Atherton, M.P.; Cobbing, E.J.; Bekinsale, R.D.; editors). *Blackie & Son Ltd.,* 328 p. Glasgow.

Coira, B.; Davidson, J.; Mpodozis, C.; Ramos, J. 1982. Tectonic and magmatic evolution of the Andes of northern Argentina and Chile. *Earth Sciences Reviews,* Vol. 18, p. 303-332.

Cox, A.; Dalrymple, G.B. 1967. Statistical analysis of geomagnetic reversal data and the precision of potassium-argon dating. *Journal of Geophysical Research,* Vol. 72, No. 10, p. 2603-2604.

Farrar, E.; Clark, A.H.; Haynes, S.J.; Quirt, G.S.; Conn, H.; Zentilli, M. 1970. K-Ar evidence for the post-Paleozoic migrations of granitic intrusion foci in the Andes of northern Chile. *Earth and Planetary Science Letters,* Vol. 9, p. 17-28.

Frutos, J. 1974. Sobre el posible control tectónico de los yacimientos de cobre porfídico en la cuenca Andina Chilena. *Revista Geológica de Chile,* No. 1, p. 103-113.

García, F. 1967. Geología del Norte Grande de Chile. *In*

Symposium sobre el Geosinclinal Andino. *Sociedad Geológica de Chile,* 138 p. Santiago.

Godoy, E.; Davidson, J. 1976. Pilares tectónicos en compresión de edad miocena superior en los Andes del Norte de Chile. *In Congreso Geológico Chileno, No. 1, Actas,* Vol. 1, p. B87-B103. Santiago.

Gustafson, L.B.; Hunt, J.P. 1975. The porphyry copper deposit at El Salvador, Chile. *Economic Geology,* Vol. 70, p. 875-912.

Handschumacher, D.W. 1976. Post-Eocene plate tectonics of the eastern Pacific. *American Geophysical Union. Geophysical Monograph,* No. 19, p.177-202.

Heidrick, T.L.; Titley, S.R. 1982. Fracture and dike patterns in Laramide plutons and their structural and tectonic implications. *In* Advances in geology of the porphyry copper deposits, southwestern North America (Titley, S.R.; editor). *The University of Arizona Press,* p. 73-91. Tucson.

Hildreth, W. 1981. Gradients in silicic magma chambers: implications for lithospheric magmatism. *Journal of Geophysical Research,* Vol. 86, p. 10153-10192.

Hunt, J.P.; Bratt, J.A.; Marquardt, L.; J.C. 1983. Quebrada Blanca, Chile: and enriched porphyry copper deposits. *Mining Engineering,* Vol. 35, p. 636-544.

Jordan, T.E.; Isacks, B.L.; Allmendinger, R.W.; Brown, J. A.; Ramos, V.A.; Ancho, C.J. 1983. Andean tectonics related to geometry of subducted Nazca plate. *Geological Society of America, Bulletin,* Vol. 94, p. 341-361.

Jordan T.E.; Allmendinger, R.W. 1986. The Sierras Pampeanas of Argentina: A modern analogue of Rocky Mountains foreland deformation. *American Journal of Science,* Vol. 286, p. 737-764.

Lahsen, A. 1982. Upper Cenozoic volcanism and tectonism in the Andes of Northern Chile. *Earth Science Review,* Vol. 18, p. 258-302.

Maksaev V.; Moscoso, R.; Mpodozis, C.; Nasi C. 1984. Las unidades volcánicas y plutónicas del Cenozoico Superior en la Alta Cordillera del Norte Chico (29-31°S): Geología, alteración hidrotermal, y mineralización. *Revista Geológica de Chile,* No. 21 p. 11-51.

Megard, F., 1978. Etude géologique des Andes du Pérou Central. *Office de la Recherche Scientifique et Technique Outre-Mer, Memoires ORSTOM,* No. 86, 310 p.

Mercado, M. 1978. Hojas Chañaral y Potrerillos, Región de Atacama, Chile. *Instituto de Investigaciones Geológicas, Mapa Geológico Preliminar de Chile,* No. 1, 13 p.

Mercado, M. 1983. Hoja Laguna del Negro Francisco, Región de Atacama. *Servicio Nacional de Geología y Minería, Carta Geológica de Chile,* No. 56, 73 p.

Mon, R. 1976. La tectónica del borde oriental de los Andes en las provincias de Salta, Tucumán y Catamarca, República Argentina. *Asociación Geológica Argentina, Revista,* Vol. 31, p. 65-72.

Mon, R. 1979. Esquema tectónico de los Andes del norte Argentino. *Asociación Geológica Argentina, Revista,* Vol. 34, p. 53-60.

Mpodozis, C.; Davidson, J. 1979. Observaciones tectónicas en la Precordillera de Copiapó: el sector de Puquios, Sierras La Ternera Varillar. *In Congreso Geológico Chileno, No. 2, Actas,* Vol. 1, p. B111-B145. Arica.

Mpodozis, C.; Ramos, V. (in press). The Andes of Chile and Argentina. Circum-Pacific Council for Energy and Mineral Resources, Santiago, Chile.

Müller, M.G.; Perelló, L.J. 1982. Geología regional y bioestratigrafía del Jurásico marino al occidente del Salar de Pedernales (26°15'-26°24'S; 69°16'-69°30'W). Región de Atacama, Chile. Memoria de Título (inédito). *Universidad de Chile, Departamento de Geología,* 316 p. Santiago.

Muzzio, G. 1980. Geología de la región comprendida entre el Cordón El Varillar y Sierra de Vizcachas, Precordillera de Atacama, Chile. Memoria de Título (inédito). *Universidad de Chile, Departamento de Geología,* 176 p. Santiago.

Naranjo, J.A.; Puig, A. 1984. Hojas Taltal y Chañaral, Regiones de Antofagasta y Atacama. *Servicio Nacional de Geología y Minería, Carta Geológica de Chile,* No. 62-63, 140 p.

Ode, H. 1957. Mechanical analysis of the dike pattern of the Spanish Peaks area, Colorado. *Geological Society of America, Bulletin,* Vol. 68, p. 567-576.

Olson, S.F. 1984. Geology of the Potrerillos District, Atacama, Chile. Unpublished Ph.D. Thesis. Stanford University, 190 p. Stanford, California.

Pardo-Casas, F.; Molnar, P. 1987. Relative motion of the Nazca (Farallon) and South American Plates since Late Cretacous time. *Tectonics,* Vol. 6, No. 3, p. 233-248.

Parra, A.M. 1983. Petrografía y petrología de los cuerpos intrusivos de la mina Potrerillos, Región de Atacama. Memoria de Título (inédito). *Universidad de Chile, Departamento de Geología y Geofísica,* 154 p. Santiago.

Perelló, J.; Müller, G. 1984. El horst de Sierra Castillo en la Cordillera de Domeyko, al occidente del Salar de Pedernales: sus fallas límites Barrancas y Sierra Castillo. *Comunicaciones,* No. 34, p. 47-55.

Pérez, E. 1982. Bioestratigrafía del Jurásico de Quebrada Asientos, norte de Potrerillos, Región de Atacama. *Servicio Nacional de Geología y Minería, Boletín,* No. 37, 149 p.

Quirt, S.; Clark, A.H. Farrar, E.; Sillitoe, R.H. 1971. Potassium-argon ages of porphyry copper deposits in northern and central Chile. *Geological Society of America, Abstracts and Programs,* Vol. 3, p. 676-677.

Reed, E.F. 1932. Unpublished map of the Potrerillos district. *Andes Copper Mining Co.* Potrerillos, Chile.

Reutter, K.J. 1974. Entwicklung und Bauplan der chilenischen Hochkordillere im Bereich 29° südlicher Breite. *Neues Jahrbuch für Geologie und Palaontologie Abhanlungen,* Vol. 146, No. 2, p. 153-178.

Ruiz, C.; Corvalán, J., Klohn, C.; Klohn, E.; Levi, B

1965. Geología y yacimientos metalíferos de Chile. *Instituto de Investigaciones Geológicas*, 360 p. Santiago.

Segerstrom, K. 1967. Geology and ore deposits of central Atacama province, Chile. *Geological Society of America, Bulletin*, Vol 78, p. 305-318.

Sepúlveda, P.; Naranjo, J.A. 1982. Hoja Carrera Pinto, Región de Atacama. *Servicio Nacional de Geología y Minería, Carta Geológica de Chile*, No. 53, 62 p.

Servicio Nacional de Geología y Minería. 1982. Mapa Geológico de Chile, 1:1.000.000 (Escobar, F.; editor). *Instituto Geográfico Militar*, 6 hojas.

Sillitoe, R.H. 1973. Tops and bottoms of porphyry copper deposits. *Economic Geology*, Vol. 68, p. 799-815.

Sillitoe, R.H. 1976. Andean mineralization: a model for the metallogeny of convergent plate margins. *Geological Association of Canada, Special Paper*, No. 14, p. 59-100.

Sillitoe, R.H. 1981. Regional aspects of the Andean porphyry copper belt in Chile and Argentina. *Institute Mining and Metallurgy Transactions*, Vol. 90, p. B15-B36.

Tilling, R.I. 1976. El batolito andino cerca de Copiapó, Provincia de Atacama. Geología y Petrología. *Revista Geológica de Chile*, Vol. 3, No. 1, p. 1-24.

Tobar, A. 1978. Stratigraphy and structure of the El Salvador-Potrerillos region, Atacama, Chile. Unpubished Ph.D. Thesis. *University of California*, 117 p. Berkeley, California.

Zeil, W. 1979. The Andes, a geological review. *Gebruder Borntraeger*, 260 p. Berlin.

Zentilli, M. 1974. Geological evolution and metallogenetic relationships in the Andes of northern Chile between 26° and 29°S. (Unpublished Ph.D. Thesis). *Queens University*, 446 p. Kingston, Ontario.

APPENDIX 1. SAMPLE LOCATIONS

Sample Number	UTM Coordinates North	East	Comments
Table 1			
DC-1	7062.560	462.580	6 km ESE of Cerro El Hueso
DC-27	7071.260	458.440	Underground, Las Vegas adit
DC-28	7071,290	458.355	Underground, Las Vegas adit
DC-29	7071.330	458.250	Underground, Las Vegas adit
Table 2			
CH3-1	7070.700	456.100	Ridge north of Cerro San Antonio
DC-17	7068.840	461.630	1 km al ENE of Silica mine
DC-19	7068.840	461.870	2.5 km N25°E of Silica mine
DC-14	7070.200	456.230	Ridge north of Cerro San Antonio
DC-33	7069.800	452.560	Quebrada Cajoncito
DC-36	7070.860	452.420	Quebrada Cajoncito
CH3-5	7062.850	448.360	Vega Primera, near Cerro Vicuña
Table 3			
DC-2	7066-440	461.400	4 km west of Cerro El Hueso
CH3-1	7070.700	456.100	Ridge north of Cerro San Antonio
DC-43	7063.550	449.500	East of Cerro Vicuña
CH3-5	7062.850	448.360	Vega Primera, near Cerro Vicuña
CH3-10	7072.000	463.600	5.5 km ENE of Cobre Porphyry
DC-7	7070.190	468.780	2.5 km E of Cobre Porphyry
SNA	7070.600	457.530	Underground, Las Vegas level
DC-8	7065.380	457.190	Cerro El Hueso
DC-9	7065.180	457.100	Cerro El Hueso
Table 5			
DC-21	7071.750	457.810	North Porphyry
DC-9	7065.180	457.100	Cerro El Hueso
DC-3	7064.100	459.200	2 km ESE of Cerro El Hueso